

Review

# State-of-Art Review of NO Reduction Technologies by CO, CH<sub>4</sub> and H<sub>2</sub>

Jialin Song <sup>1,†</sup>, Ziliang Wang <sup>2,†</sup>, Xingxing Cheng <sup>1,\*</sup> and Xiuping Wang <sup>1</sup>

<sup>1</sup> National Engineering Laboratory for Reducing Emissions from Coal Combustion, School of Energy and Power Engineering, Shandong University, Jinan 250061, China; songjialin199@163.com (J.S.); wangxiupingw@163.com (X.W.)

<sup>2</sup> Innovation Centre, BC Research Inc., 12920 Mitchell Rd, Richmond, BC V6V 1M8, Canada; ziliangwang053@gmail.com

\* Correspondence: xcheng@sdu.edu.cn; Tel.: +86-531-8839-9372 (ext. 615)

† Co-first author. These authors contributed equally to this work.

**Abstract:** Removal of nitrogen oxides during coal combustion is a subject of great concerns. The present study reviews the state-of-art catalysts for NO reduction by CO, CH<sub>4</sub>, and H<sub>2</sub>. In terms of NO reduction by CO and CH<sub>4</sub>, it focuses on the preparation methodologies and catalytic properties of noble metal catalysts and non-noble metal catalysts. In the technology of NO removal by H<sub>2</sub>, the NO removal performance of the noble metal catalyst is mainly discussed from the traditional carrier and the new carrier, such as Al<sub>2</sub>O<sub>3</sub>, ZSM-5, OMS-2, MOFs, perovskite oxide, etc. By adopting new preparation methodologies and introducing the secondary metal component, the catalysts supported by a traditional carrier could achieve a much higher activity. New carrier for catalyst design seems a promising aspect for improving the catalyst performance, i.e., catalytic activity and stability, in future. Moreover, mechanisms of catalytic NO reduction by these three agents are discussed in-depth. Through the critical review, it is found that the adsorption of NO<sub>x</sub> and the decomposition of NO are key steps in NO removal by CO, and the activation of the C-H bond in CH<sub>4</sub> and H-H bonds in H<sub>2</sub> serves as a rate determining step of the reaction of NO removal by CH<sub>4</sub> and H<sub>2</sub>, respectively.

**Keywords:** NO reduction; catalyst; carbon monoxide; methane; hydrogen



**Citation:** Song, J.; Wang, Z.; Cheng, X.; Wang, X. State-of-Art Review of NO Reduction Technologies by CO, CH<sub>4</sub> and H<sub>2</sub>. *Processes* **2021**, *9*, 563. <https://doi.org/10.3390/pr9030563>

Academic Editor: Olivier Monfort

Received: 14 February 2021

Accepted: 16 March 2021

Published: 23 March 2021

**Publisher's Note:** MDPI stays neutral with regard to jurisdictional claims in published maps and institutional affiliations.



**Copyright:** © 2021 by the authors. Licensee MDPI, Basel, Switzerland. This article is an open access article distributed under the terms and conditions of the Creative Commons Attribution (CC BY) license (<https://creativecommons.org/licenses/by/4.0/>).

## 1. Introduction

Coal is an important basic energy and a raw material for chemicals in China. Nitrogen oxide (NO<sub>x</sub>), a pollutant of coal combustion, causes a tremendously negative impact on ecosystems and human health. Although researchers have recently made great progress in NO<sub>x</sub> reduction, there are still numerous challenges to remove NO<sub>x</sub> completely and efficiently from the combustion flue gas.

The catalytic removal of NO<sub>x</sub> under lean-burn conditions is one of the most important targets in catalysis research [1]. The most widely used NO removal technology in current coal-fired power plants is the Selective Catalytic Reduction (SCR) technology due to its stable, high efficiency and superior performance. This technology commonly uses ammonia (NH<sub>3</sub>), carbon monoxide (CO), methane (CH<sub>4</sub>), and hydrogen (H<sub>2</sub>) as reducing agents. Within those reductants, SCR of NO<sub>x</sub> with NH<sub>3</sub> (NH<sub>3</sub>-SCR) is a widely commercialized technology for NO<sub>x</sub> removal from stationary sources. Urea is often chosen as an alternative reducing agent, because it can be hydrolyzed to generate NH<sub>3</sub>. However, hydrolysis of urea is prone to form explosive ammonia salts, which further can likely block the channels and deactivate catalyst. Figure 1 illustrates a schematic process of NH<sub>3</sub>-SCR technology. At a relative low temperature, NH<sub>3</sub> will react with sulfur dioxide (SO<sub>2</sub>) in the flue gas to form ammonium sulfite ((NH<sub>4</sub>)<sub>2</sub>SO<sub>3</sub>), ammonium bisulfate (NH<sub>4</sub>HSO<sub>4</sub>), etc., which are thick and sticky components and easily clog the piping. For this reason, the heavy metal catalyst vanadium oxide (V<sub>2</sub>O<sub>5</sub>) is traditionally employed in NH<sub>3</sub>-SCR technology

to convert  $\text{SO}_2$  to  $\text{SO}_3$ , but the spent catalyst is hard to handle. In addition, the commercial catalyst requires higher than  $350\text{ }^\circ\text{C}$  temperature to keep its catalytic activity.  $\text{NH}_3$ -SCR technology with different catalysts has been reviewed by others [1–3].

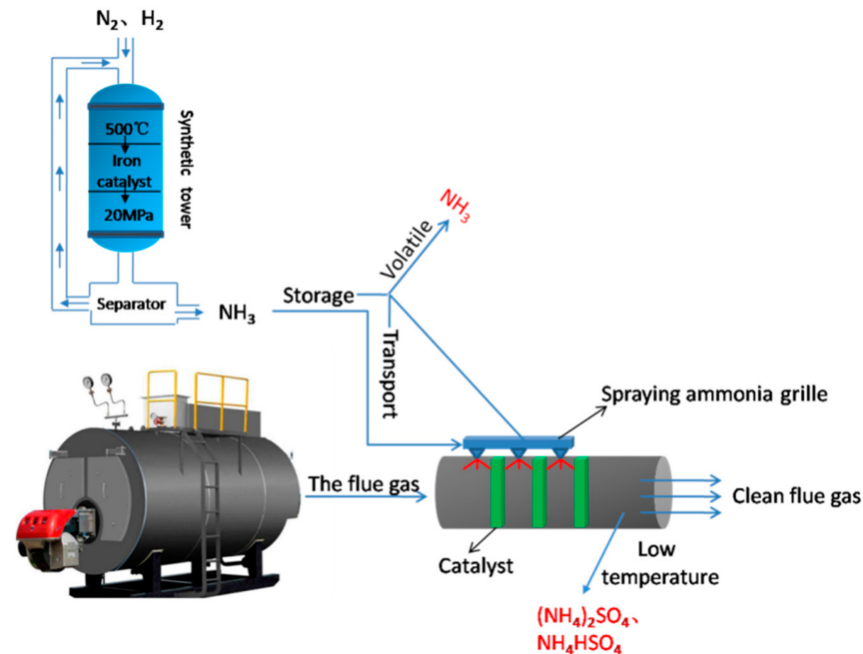
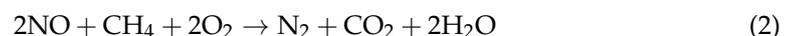


Figure 1. A schematic process of  $\text{NH}_3$ -SCR of  $\text{NO}_x$ .

Since forementioned concerns in  $\text{NH}_3$ -SCR technology, researchers start to explore other reducing agents, such as  $\text{CO}$ ,  $\text{CH}_4$ , and  $\text{H}_2$ . Initially, most researchers chose noble metals as active components due to their superior catalytic performance. However, recently, transition metal catalysts have attracted great interest and shown exciting results. Meanwhile, compared to the noble metal catalyst, cost-effective transition metal catalysts seem more promising [4–6].

The main reactions of  $\text{NO}$  reduction by  $\text{CO}$  ( $\text{CO}$ -SCR),  $\text{CH}_4$  ( $\text{CH}_4$ -SCR), and  $\text{H}_2$  ( $\text{H}_2$ -SCR) over different catalysts are



Except catalyst, these reactions are affected by the concentration of  $\text{NO}$  and  $\text{O}_2$  in the feed gas stream [7–9], the temperature of reaction [10,11], water content [12,13], and sulfur, [14,15] etc. In these three technologies, the key step is the decomposition of adsorbed  $\text{NO}$  to produce adsorbed  $\text{N}_2\text{O}$ . The  $\text{N}_2\text{O} + \text{CO}$  reaction in  $\text{CO}$ -SCR is faster than the isolated  $\text{N}_2\text{O} + \text{CO}$  reaction over  $\text{Rh}/\text{Al}_2\text{O}_3$  by an order of magnitude [16]. In  $\text{CH}_4$ -SCR, the activation of the C-H bond in  $\text{CH}_4$  serves as a rate determining step of the reaction of  $\text{NO}$  removal by  $\text{CH}_4$  [17]. In  $\text{H}_2$ -SCR,  $\text{H}_2$  dissociation to atomic H is more difficult due to high-energy barrier and endothermicity [18]. Hong et al. [10] found that  $\text{NO}$  can hardly be oxidized to  $\text{NO}_2$  at low temperatures. First, the gas phase  $\text{NO}$  is adsorbed by the surface of Pt; then, the adsorbed  $\text{NO}$  reacts with the adsorbed O to form a nitrate species. The adsorbed H migrates from the Pt surface to the Pt carrier interface through the H overflow, and then reacts with  $\text{NO}^{\delta+}$  and  $\text{NO}^{3-}$  to form  $\text{N}_2$ . In the high temperature range,  $\text{NO}$  is partially oxidized to  $\text{NO}_2$ .  $\text{NO}_2$  acts as an active intermediate in the  $\text{NO}_x$  reduction reaction. In the presence of  $\text{NO}_2$ , N adsorbed at the Pt position reacts with active H to form  $\text{NH}^{4+}$  species, which then react with  $\text{NO}$  and  $\text{O}_2$  to form  $\text{N}_2$ .

Oxygen in the flue gas plays an important role in NO<sub>x</sub> removal by CO-SCR, CH<sub>4</sub>-SCR, and H<sub>2</sub>-SCR. Oxygen preferentially oxidizes CO to CO<sub>2</sub> and inhibits CO-NO reaction to reduce NO removal efficiency in the CO-SCR process [19,20]. However, in the CH<sub>4</sub>-SCR process, the inhibition of oxygen is different from that of CO-NO reaction; oxygen plays a dual role of positive (promoting adsorption) and negative (suppressing reduction) in the NO reaction process [7,8]. The negative effect of oxygen on NO removal efficiency stems from the competitive reaction of oxygen and NO with respect to CH<sub>4</sub>, and the oxygen in the flue gas is an essential factor for the oxidation of NO to the catalyst surface. Therefore, a suitable catalyst should be selected to react methane with NO to increase the conversion rate of NO. In the H<sub>2</sub>-SCR process [9], oxygen preferentially reacts with H<sub>2</sub> to form water due to its lower energy barrier ( $\Delta H^0 = -242$  kJ/molH<sub>2</sub>) compared to the reaction of two NO molecules with four hydrogen molecules to form N<sub>2</sub> and water ( $\Delta H^0 = -574$  kJ/molH<sub>2</sub>), as shown in Equation (3). It results in poor activity and selectivity toward N<sub>2</sub>.

In the paper, the latest research progress of NO removal with CO (CO-SCR), CH<sub>4</sub> (CH<sub>4</sub>-SCR), and H<sub>2</sub> (H<sub>2</sub>-SCR) are comprehensively reviewed. The precious and non-precious catalysts for NO<sub>x</sub> removal with CO and CH<sub>4</sub> reductants are reviewed. In terms of H<sub>2</sub>-SCR, we focus on catalyst carrier. Moreover, their reaction mechanisms under different reducing agents are critically discussed. Finally, based on the discussions of effect factors and reaction mechanism, a preliminary outlook for SCR of NO has been proposed.

## 2. Catalysts for NO Removal by CO

Among these three approaches, NO reduction by CO has attracted great interest, because it removes two harmful gases, namely NO and CO, simultaneously [4,21]. CO is one of product in the flue gas and can be directly produced by pulverized coal gasification or pyrolysis. More important, it is not easy to form carbon in the process of NO removal by CO and decrease the catalyst deactivation due to carbon deposition. As a reducing agent, CO is not involved in any clogging problems like ammonia is. These advantages have made CO become the current flue gas NO<sub>x</sub> removal research hotspot.

In the technology of NO removal by CO, catalysts can be divided into two types: precious and non-precious metal catalysts. The former shows higher NO removal efficiency when the temperature is low, but the temperature window is narrow and the price is high. The preparation cost of the latter is significantly lower than that of the former, but the NO removal efficiency is relatively lower. At present, many researchers are committed to finding high performance and cost-effective non-precious NO removal catalysts. Table 1 lists some of catalysts for CO catalytic reduction of NO<sub>x</sub> under different conditions.

### 2.1. Precious Metal Catalyst

Most studies conducted by the early researchers utilized precious metal as active site in the catalysts for NO removal by CO, and the experiments proved that precious metal catalyst has superior performance in NO removal. If only precious metals are used, this is no surprise for high or even extremely high experimental cost, which hinders the normal experiment operation. Later, scientists switched to dope a precious metal as an active component on a carrier, which is proven as an effective means with significantly lower metal consumption and excellent catalytic activity. Noble metals such as platinum (Pt), palladium (Pd), rhodium (Rh), and ruthenium (Ru) are reported to have superior catalytic effect on the reaction of NO removal by CO, and their catalytic effect follows a general order of Ru > Rh > Pt > Pd.

Presence of noble metal in the catalyst can improve the NO reduction efficiency in the CO-SCR technology. Cobalt oxide catalysts are used in NO reduction by CO because of their good catalytic activity [22]. Salker et al. [23] used citric acid assisted sol-gel method to prepare Pd, Rh, and Ru doped cobalt oxide spinel and obtain nano-catalyst. They found that the presence of precious metals increases the activity and stability of the catalyst, and the doped noble metal contributes to the adsorption of NO and promoted

the reduction of NO to N<sub>2</sub>. The order of activity is Rh<sub>0.05</sub>Co<sub>2.95</sub>O<sub>4</sub> > Pd<sub>0.05</sub>Co<sub>2.95</sub>O<sub>4</sub> > Ru<sub>0.05</sub>Co<sub>2.95</sub>O<sub>4</sub> > Co<sub>3</sub>O<sub>4</sub>.

Compared with the unsupported catalyst, the catalyst obtained by dispersing the metal (Mn, Ru, Pd, Pt) on the metal oxide (CeO<sub>2</sub>, TiO<sub>2</sub>, ZnO) has excess adsorption vacancies and higher oxidation activity [24]. Chao et al. [25] used sol-gel methods to prepare La<sub>1.6</sub>Ba<sub>0.4</sub>NiO<sub>4</sub> and Ru/La<sub>1.6</sub>Ba<sub>0.4</sub>NiO<sub>4</sub> catalysts. The experiments were carried out under the conditions of 5000 ppm NO and 5000 ppm CO. The test results showed that the efficiency of the latter is significantly higher than that of the former. The characterization results indicated that the interaction between Ru and the perovskite support leads to an increase in the reduction of the catalyst, which in turn increases the conversion of NO. Oton et al. [26] prepared solid catalysts by dispersing Pt, Co, Fe, and Ni nanoparticles on alumina. They found that the Pt/Al<sub>2</sub>O<sub>3</sub> catalyst has a better performance than those of Ni, Fe, and Co supported counterparts. However, NiPt/Al<sub>2</sub>O<sub>3</sub> catalyst can promote CO-SCR reaction performance at relatively low temperatures due to the interaction and synergy between Pt (Ni) nanoparticles and its carrier. The reason is that the electron transfer between the PtO<sub>x</sub>(Ni) and chlorinated Pt species on the support provides a more active solid in the CO-SCR reaction.

The composite support can increase the activity of the catalyst. Wu et al. [27] synthesized TiO<sub>2</sub>/γ-Al<sub>2</sub>O<sub>3</sub> supported In/Ag catalyst by impregnation method. Results of microscopic structure and surface properties tests of the catalyst showed that the catalyst has high dispersion, large amounts of surface active components, and high NO adsorption capacity. The introduction of TiO<sub>2</sub> into the γ-Al<sub>2</sub>O<sub>3</sub> support leads to an increase in NO adsorption and more uniform dispersion of In species and Ag species. Ag species not only stabilizes, but also enhances In species dispersion in the catalyst. Therefore, TiO<sub>2</sub>/γ-Al<sub>2</sub>O<sub>3</sub> supported In/Ag catalyst appeals to a good performance and stability for the NO reduction by CO. Cerium dioxide (CeO<sub>2</sub>) is a very important rare earth oxide material with excellent oxygen storage and release. Ilieva et al. [28] synthesized Fe-modified CeO<sub>2</sub> carrier by two different methods of mechanochemical mixing (MM) and impregnation (IM) methods, and doped 3 wt.% nanosized gold (Au) thereon by deposition precipitation method. The performance test results showed that the presence of nanosized Au particles is not of crucial importance, but Fe-modification of CeO<sub>2</sub> promotes NO reduction performance. However, the efficacy of Fe-modification decreases the selectivity by increasing the selectivity to nitrous oxide (N<sub>2</sub>O). Moreover, an addition of a new support to a single support can increase the activity of the supported catalyst. Huang et al. [29] compared Pt catalysts supported on TiO<sub>2</sub> and CeO<sub>2</sub>-TiO<sub>2</sub> for the NO reduction by CO with ultraviolet light irradiation. The doped CeO<sub>2</sub> can strengthen the electron transfer from TiO<sub>2</sub> to Pt through a process of Ce<sup>4+</sup> → Ce<sup>3+</sup> under UV irradiation, resulting in the adsorption and activation of CO and NO species at Pt/CeO<sub>2</sub>-TiO<sub>2</sub>. Compared to Pt/TiO<sub>2</sub>, Pt/CeO<sub>2</sub>-TiO<sub>2</sub> has higher thermal catalytic activity and stability for NO removal by CO. They also stated that the photo-excitation of supports can enhance the strong interaction between nanosized Pt particles and support, and improve the thermo-catalytic reactivity of catalysts. Ferrer V et al. [30] doped Pd on Ce<sub>0.73</sub>Tb<sub>0.27</sub>O<sub>x</sub>/SiO<sub>2</sub>, Ce<sub>0.6</sub>Zr<sub>0.4</sub>O<sub>x</sub>/SiO<sub>2</sub>, Ce<sub>0.73</sub>Tb<sub>0.27</sub>O<sub>x</sub>/La<sub>2</sub>O<sub>3</sub>-Al<sub>2</sub>O<sub>3</sub>, and Ce<sub>0.6</sub>Zr<sub>0.4</sub>O<sub>x</sub>/La<sub>2</sub>O<sub>3</sub>-Al<sub>2</sub>O<sub>3</sub> for the reduction of NO by CO. Temperature-programmed reduction results indicated that Tb or Zr incorporation improves the reducibility and oxygen storage capacity. CO chemisorption data suggested the presence of large PdO particles due to the low CO/Pd ratio. No significant differences were obtained in light off temperatures for all Pd catalysts, and the most active catalyst was 1.5%Pd/Ce<sub>0.6</sub>Zr<sub>0.4</sub>O<sub>x</sub>/SiO<sub>2</sub>.

Some novel catalyst preparation methods have been applied to boost the activity of existing catalysts. Wang et al. [31] introduced an evaporation induced self-assembly (EISA) method to produce a catalyst under a triblock copolymer as a soft template. First, 3 wt.% Au was deposited on the mesoporous Al-Ti mixed oxide to obtain the parent Au/AlTiO<sub>x</sub> catalyst, and then CeO<sub>x</sub> was impregnated thereon to prepare catalyst with Au:Ce molar ratios of 4:1, 2:1, and 1:1, respectively. Au/AlTiO<sub>x</sub> catalyst showed a very low activity,

but the Au-Ce(2:1)/AlTiO<sub>x</sub> catalyst resulted in a NO conversion of 100% under the same conditions. Shin et al. [32] assembled 2–16 nm Pd-Au nanoparticles into TiO<sub>2</sub> nanofibers with  $117 \pm 68$  nm diameter by means of electrospinning method. The synthesized Pd-Au/TiO<sub>2</sub> fiber catalyst shows a greater reactivities for the NO reduction with CO than Pd and Au alone fiber media because of decreased activation energies in the Arrhenius expression. In addition, the catalyst performance can be modified and improved by adding a plurality of different metals. For aluminum-supported catalysts, the addition of barium significantly inhibits the sintering of alumina, improves the dispersibility of Pd, and promotes the formation of active surface nitrates. It has higher catalytic activity than barium-free Pd/Al<sub>2</sub>O<sub>3</sub> catalysts [33].

In contrast with most other works, Higo et al. [12] found that water only slightly affected CO and NO adsorption on PdLa<sub>0.9</sub>Ba<sub>0.1</sub>AlO<sub>3-δ</sub> catalyst surface and improved the carbonate species generated to rapidly remove. In addition to the contribution from lattice oxygen and oxygen vacancy on that catalyst, the occurrence of water was beneficial for NO removal by CO at low temperature (200 °C or below).

## 2.2. Non-Precious Metal Catalyst

### 2.2.1. Effect of Preparation Method

In the technology of NO removal by CO, iron oxide (Fe<sub>2</sub>O<sub>3</sub>), alumina (Al<sub>2</sub>O<sub>3</sub>), silica (SiO<sub>2</sub>), and ceria (CeO<sub>2</sub>), ZSM-5 are the commonly used carriers. In the process of catalyst preparation, diluted nitric acid is often used to react with the oxide carrier to modify the surface structure of the carrier particles, while hydrothermal method can provide the precursor with physical and chemical environments that cannot be obtained under atmospheric conditions. Sun et al. [34] prepared a series of CeO<sub>2</sub> modified CuO/γ-Al<sub>2</sub>O<sub>3</sub> catalysts by stepwise impregnation (SI) and co-impregnation (CI). These two different preparation methods induce significant difference on the spatial distribution of Cu species and in turn lead to different catalytic activity for NO reduction by CO. Compared to CuCeAl-CI, in CuCeAl-SI, more Cu species are dispersed on the surface of CeO<sub>2</sub>, fewer Cu particles are distributed on γ-Al<sub>2</sub>O<sub>3</sub>, and far fewer Cu species are migrated into ceria lattice during the calcination process. The activity of CuCeAl-SI was proven to be higher than that of CuCeAl-CI in NO reduction by CO, because sufficient interfacial CuO-CeO<sub>2</sub> species are provided via the stepwise impregnation method.

### 2.2.2. Effect of Doped Species and Its Loading

The active species distribution can be affected by their precursor. Zhang et al. [35] tried copper and cobalt (acetate and nitrate) precursors to prepare CuO-CoO<sub>x</sub>/γ-Al<sub>2</sub>O<sub>3</sub> catalysts via the co-impregnation method. With copper or cobalt acetate precursor, the Cu/Co particles are in an agglomerated state and have low activity; while with copper or cobalt nitrate, the metal particles are well dispersed and have high activity. Cha et al. [36] demonstrated that the post-annealing process, namely annealing temperature and time, also can affect the catalyst-support interaction. In the preparation of Fe-oxide/Al<sub>2</sub>O<sub>3</sub> catalyst by means of temperature-adjusted chemical vapor deposition by depositing nano-sized Fe-oxide particles with a lateral size less than 2 nm in mesoporous Al<sub>2</sub>O<sub>3</sub>, the interface between Fe-oxide and Al<sub>2</sub>O<sub>3</sub> is significantly enhanced and consequently enhances the catalytic activity for the NO reduction by CO. Boningari et al. [37] synthesized a series of anatase titania supported transition metal oxide (M = Cr, Mn, Fe, Ni, Cu; 10 wt.%) catalysts by means of wet impregnation method. Under identical operating conditions, MnO<sub>x</sub>/TiO<sub>2</sub> catalyst shows a better performance of NO removal compared to the other catalysts, and exhibits higher than 90% NO conversion even in the presence of oxygen and at 50,000 h<sup>-1</sup> high space velocity.

The loading of the active component affects the activity of the catalyst. A series of Fe-Ba/ZSM-5 catalysts with various Fe loadings (2.7–10 wt.%) were prepared via the impregnation method for NO and O<sub>2</sub> adsorption and NO reduction by CO at 250–400 °C by Zhang et al. [38]. Results of NO-CO activity tests illustrated that the NO removal

efficiency is greatly influenced by  $\alpha$ -Fe<sub>2</sub>O<sub>3</sub> species and its distribution degree. Higher Fe loadings, mainly  $\alpha$ -Fe<sub>2</sub>O<sub>3</sub>, lead to an increased amount of adsorbed NO<sub>x</sub> and more uniform Fe species distribution, resulting in a better catalytic activity. However, the NO<sub>x</sub> adsorption capacity was observed to decrease at Fe loadings above 8.3% due to aggregation, and 4.7 wt.% Fe loading Fe-Ba/ZSM-5 catalysts exhibited the best NO<sub>x</sub> reduction efficiency.

### 2.2.3. Effect of CeO<sub>2</sub>

CeO<sub>2</sub> has high storage and oxygen release capacity. As an active carrier, CeO<sub>2</sub> has a high energy surface and can effectively improve the dispersibility of the active component and the stability of the catalyst through synergistic action. However, pure CeO<sub>2</sub> has poor thermal stability and a small specific surface area, which is not suitable for industrial applications. Loading a metal, such as Mn, Cr-Cu, Co, etc., on CeO<sub>2</sub> can increase its oxygen vacancies, which in turn increases its catalytic activity. Deng et al. [4] used co-precipitation methods to prepare a variety of catalysts including CeO<sub>2</sub>, Cu/CeO<sub>2</sub>, CeMn-5:2, and Cu/CeMn- (20:1, 10:1, 5:1, 5:2, 5: 3, 5:4). They found that appropriate doping MnO<sub>x</sub> into the lattice of CeO<sub>2</sub> can increase the specific surface area, promote the catalytic activity and thermal stability, and obtain more Cu<sup>+</sup> and Ce<sup>3+</sup> (which may generate more oxygen vacancies). Cu/CeMn-10:1 exhibits the best catalytic activity of NO reduction by CO. Yoshida et al. [39] elucidated that co-doping Cr-Cu on CeO<sub>2</sub> followed by thermally aging can produce a superior catalyst for NO reduction by CO, which was not observed for monometallic Cr or Cu catalyst and bulk oxide (CuCrO<sub>2</sub>). The high catalytic activity is associated with local structures of Cu<sup>+</sup> and Cr<sup>3+</sup> formed onto CeO<sub>2</sub> surface by thermal aging. The catalyst is even superior to Rh/CeO<sub>2</sub> with similar 0.14 wt.% metal loading and thermal aging history.

The catalyst activity of cerium oxide supported transition metal oxides formation is highly dependent on its synthesis parameters such as oxygen vacancy concentration and metal precursor selection. Savereide et al. [40] synthesized CoO<sub>x</sub>/CeO<sub>2</sub> catalyst by incipient wetness impregnation method with different Co precursors, namely cobalt (II) nitrate hexahydrate, cobalt (II) acetate, cobalt (III) acetylacetonate, and disodium cobalt (II) on the CeO<sub>2</sub> nanorods and commercial nanoparticles. They mainly found that the CeO<sub>2</sub> nanorods is better than the commercial CeO<sub>2</sub> nanoparticles due to greater number of defects in nanorods consistent with better anchoring at the oxygen vacancy defects, and the cobalt (III) acetylacetonate outperforms other precursors. They thus suggested that the reactivity of the supported CoO<sub>x</sub> on the NO reduction by CO are essentially affected by the precursor choice and defected supports. The same phenomena was also observed on  $\gamma$ -Al<sub>2</sub>O<sub>3</sub> supported catalyst. Wang et al. [41] prepared CuO/MnO<sub>x</sub>/ $\gamma$ -Al<sub>2</sub>O<sub>3</sub> catalyst with acetate and nitrate precursors to reduce NO by CO. The catalyst prepared from acetate precursors (Cu/Mn/Al-A) was observed to have better catalytic activity than nitrate derived catalyst (Cu/Mn/Al-N), because Mn species are more uniformly dispersed on the catalyst surface. For both catalysts, the state of copper is similar, while obvious difference is represented by the chemical valence of manganese species. Mn (III) is enriched on  $\gamma$ -Al<sub>2</sub>O<sub>3</sub> by using manganese acetate as a precursor, while Mn (IV) is dominated when manganese nitrate is employed. In our opinion, low-oxidization-state metal ion favors metal oxide dispersion, which consequently prompts NO dissociation and improves the performance in the NO reduction by CO.

### 2.2.4. Effect of Pretreatment Method

A proper pretreatment of the catalyst can improve its activity. Gu et al. [42] prepared CuO/CeO<sub>2</sub> catalyst by impregnation method, and carried out CO pretreatment. As a result, it was found that the activity of the catalyst after the CO pretreatment is remarkably improved. Yoshida et al. [39] used vacuum cathode pulse arc plasma technology to prepare Cr-Cu/CeO<sub>2</sub>, Cr-Cu/CeO<sub>2</sub>-ZrO<sub>2</sub>, Cr-Cu/ZrO<sub>2</sub>, Cr-Cu/Al<sub>2</sub>O<sub>3</sub>, and Cr-Cu/TiO<sub>2</sub> catalyst. The NO activity test results showed that Cr-Cu/CeO<sub>2</sub> has the highest catalytic activity. The calcination temperature also affects the performance of the prepared catalyst, especially

the physical properties. Zhang et al. [43] prepared a series of  $\text{CoO}_x$  catalysts supported by  $\text{CeO}_2$  at different firing temperatures. It was found that the physical properties (SSA, pore size, and particle size) of the catalysts change significantly with the increase of firing temperature, especially when the temperature was higher than 700 °C.

#### 2.2.5. Semi-Coke Catalyst

In our group, we have been working on activated semi-coke (ASC) supported catalysts for NO reduction by CO for many years [44,45]. The semi-coke is a by-product of lignite combustion, which has good adsorption properties and high mechanical strength. ASC doped with metals exhibits a remarkable ability for nitrogen oxides adsorption. Understanding the fact that iron oxides are not efficient at low temperatures and cobalt oxides exhibit high  $\text{N}_2\text{O}$  selectivity, we have successfully synthesized  $\text{Fe}_{0.8}\text{Co}_{0.2}/\text{ASC}$  with superior NO reduction performance by CO at low temperatures (<350 °C) via the hydrothermal method [44]. The mixed crystal effect between Fe and Co is expected to generate microstress in the lattice and consequently create some defects, which is beneficial for oxygen dissociation and oxygen vacancies generation. The characterization results specified that the Co is the catalytic site of nitrate oxide, and the Fe is the catalytic site of CO. Following this idea, we further [45] revealed that lignite-type ASC catalyst has better NO adsorption and reduction performance than the bituminous coal-type ASC catalyst.

#### 2.2.6. Non-Precious Multi-Metal/Metal Oxide Catalyst

Multi-metal/metal oxide catalyst as an emerging catalyst attracts more and more attention due to its excellent catalytic performance, better than single metal oxide catalyst. In our group, two [11] and three [46] metal oxides support catalysts were assessed to reduce NO by CO. Cheng et al. [11] found that Cu supported on mixed  $\text{Fe}_2\text{O}_3$  and  $\text{CeO}_2$  support catalyst is better than that of single metal oxide catalyst. Cubic  $\text{CeO}_2$  was found to serve as the lattice framework in the support of mixed oxides, and  $\text{Fe}_2\text{O}_3$  phases are mainly formed on the surface of  $\text{CeO}_2$  lattice.  $\text{CeO}_2$  serves as the storing sites of carbonate and enhances CO oxidation,  $\text{Fe}_2\text{O}_3$  serves as the storing sites of nitrites and nitrates and facilitates  $\text{NO}_x$  adsorption, and impregnated copper helps to convert inactive nitrites into active intermediates for NO+CO reaction. The promoted adsorption and conversion of both carbonates and nitrites/nitrates over the catalyst is likely responsible for its excellent NO reduction by CO. Moreover, Du et al. [46] prepared three composite metal oxide catalysts ( $\text{Cu}_2\text{M}_9\text{CeO}_x$ , where M = Fe, Co, Ni) by citric acid complexation. The experimental results showed that the  $\text{NO}_x$  reduction efficiency of the three catalysts is  $\text{Cu}_2\text{Co}_9\text{CeO}_x > \text{Cu}_2\text{Fe}_9\text{CeO}_x > \text{Cu}_2\text{Ni}_9\text{CeO}_x$ . The results of TEM and HRTEM unveiled that the interior of  $\text{Cu}_2\text{Co}_9\text{CeO}_x$  may be composed of CuCo mixed oxide and  $\text{Ce}_{11}\text{O}_{20}$ .

To target a low temperature application, Wang et al. [47] synthesized a series of  $\text{CuCe}_x\text{Co}_{1-x}\text{O}_y$  ( $x = 0.1, 0.2, 0.3, 0.4$ ) catalysts, which can achieve 100% NO reduction by CO on the  $\text{CuCe}_{0.2}\text{Co}_{0.8}\text{O}_y$  surface at as low as 175 °C temperature. They thought that the addition of Ce not only improves the dispersity of CuO species on the catalyst surface, but also promotes the redox properties of catalyst. All those lead to an increase in the CO adsorption/conversion, the activation of surface oxygen vacancies, and NO dissociation on the catalyst surface.

#### 2.2.7. Effect of New Carriers

Catalysts with new carriers, including crypto-manganese or manganite (OMS-2) [48], metal-organic frameworks (MOFs) [49], zeolite imidazolate skeleton (ZIF) [50], and  $\text{AlPO}_4$  [51], have shown outstanding catalytic performance in the field of NO removal by CO. OMS-2 material (also known as crypto-manganese or manganite) is based on the  $\text{MnO}_6$  octahedron shared by the edges and has a  $2 \times 2$  tunnel structure [52]. OMS-2 is a rich, low cost, and environmentally friendly material. Due to its unique structural characteristics (such as porous structure, mixed valence of Mn, easy release, and storage of lattice oxygen), it is widely used in fine chemical synthesis and environmental purification of pollutants.

Metal-organic frameworks (MOFs) are porous crystalline materials with unique advantages, including large surface areas, primarily for gas storage, separation, and catalysis. ZIF, namely zeolite imidazolate skeleton structure material, is a kind of caged structure porous crystal material. The cage structure contains up to 264 vertices in a porous network and is constructed from up to 7524 atoms. This cage structure can selectively and efficiently capture and store gases, which, coupled with its stability and the simplicity of the synthesis method, makes ZIF an excellent carrier material. Figure 2 shows the structure of OMS-2, MOFs, and ZIF. Yun et al. [48] loaded copper oxide on OMS-2 nanorods and prepared CuO/OMS-2 nanocomposites with the molar ratios of Cu/Mn of 0.148, 0.332, 0.569, and 0.886, and found that the optimum Cu/Mn molar ratio of CuO/OMS-2 nanocomposites is 0.569. With the optimum Cu/Mn molar ratio, the CuO/OMS-2 nanocomposite shows excellent catalytic activity at temperatures below 300 °C, which significantly outperform the commercial precious metal catalysts (0.84 wt.% Pd/MgO-Al<sub>2</sub>O<sub>3</sub>-SiO<sub>2</sub>). Salker et al. [53] prepared a series of Co<sub>3-x</sub>Cu<sub>x</sub>O<sub>4</sub> (where x = 0.1, 0.2, 0.4, 0.6, 0.8, and 1.0) catalysts with different Co and Cu contents by sol-gel method. The results showed that the catalytic conversion of NO and CO on the Cu-substituted cobalt oxide spinel show enhanced activity for the reaction of CO-O<sub>2</sub> and NO-CO. Co<sub>2.9</sub>Cu<sub>0.1</sub>O<sub>4</sub> could reach a complete conversion at 209 °C for NO reduction by CO. Qin et al. [49] obtained the A-Cu-BTC (A = Fe, Ni, Co, Mn) catalyst by pre-assembly method using direct ion exchange treatment then used as a precursor to synthesize AO<sub>x</sub>/CuO<sub>y</sub>/MOF under a nitrogen atmosphere at 600 °C. As per its outstanding catalytic performance, they stated that the design of the mixed node MOFs as a precursor will have a good prospect of NO removal by CO. Wang et al. [50] synthesized metal-modified Me-ZIF-67@CuO<sub>x</sub> (Me = Mn, Fe, Al, or Zn) through colloidal chemical synthesis and encapsulation method at room temperature for low-temperature NO removal by CO. At low temperature (<200 °C), the catalytic abilities on denitrification rate were above 90%. In the meantime, the ratio of Co<sup>2+</sup>/Co<sup>3+</sup> remained a high value in Me-ZIF-67@CuO<sub>x</sub>, the denitrification performance of Al-ZIF-67@CuO<sub>x</sub> was greatly improved, and Mn-ZIF-67@CuO<sub>x</sub> had the best performance in the sulfur resistance test. Kacimi et al. [51] prepared Cu/AlPO<sub>4</sub> catalysts with Cu loading of 1, 2.5, and 5 wt.% by Cu(II) ionic complex exchange. As a result, it was found that the most active catalyst is 5Cu/AlPO<sub>4</sub>, which has the most dispersed copper (II) material, and can reduce NO at a low temperature.

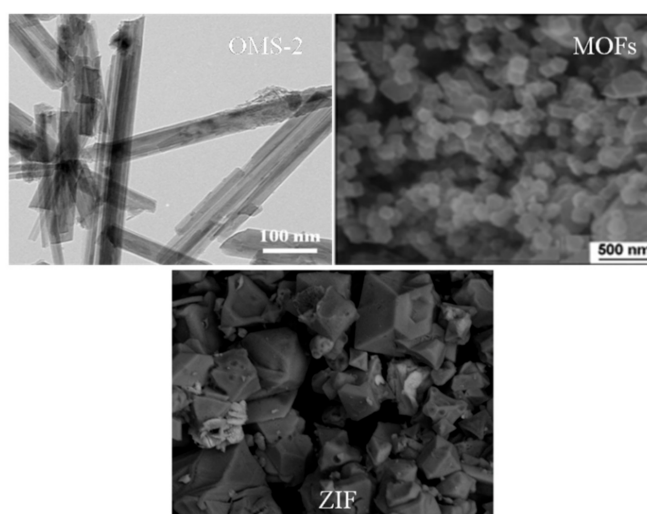


**Figure 2.** Microscopic structure of OMS-2, MOFs, and ZIF [48–50].

It is also found that some natural ores have good NO removal performance under CO atmosphere because they contain a lot of Fe, Ce, and other elements. Zhu et al. [54] investigated the catalytic denitrification performance of Bayan Obo rare earth tailings. With the synergistic effect between Fe elements, in the tailing exists mainly in the form of

$\text{Fe}_2\text{O}_3$  and  $\text{Fe}_3\text{O}_4$ , and  $\text{Ce}^{3+}$ , NO conversion rate could reach 97% in the CO atmosphere at 900 °C.

**Table 1.** Catalysts for catalytic reduction of  $\text{NO}_x$  by CO under different conditions.

Catalyst	Maximum Conversion Temperature/°C	NO Conversion Rate/%	Reducing Agent	$\text{N}_2$ Selectivity (at Maximum Conversion Temperature)/%	Active Temperature Window/°C	GHSV / $\text{h}^{-1}$	References
FeCo/ASC(CT-KOH)	250	100	2000 ppmCO	80	250–350	20,000	[45]
FeCo/ASC(CT-vapor)	350	63	2000 ppmCO	100	250–350	20,000	[45]
5Cu/AlPO <sub>4</sub>	400	85	1.5% CO		300–500	12,000	[51]
2.5Cu/AlPO <sub>4</sub>	450	38	1.5% CO		300–500	12,000	[51]
1Cu/AlPO <sub>4</sub>	450	25	1.5% CO		300–500	12,000	[51]
CuO/ $\gamma$ -Al <sub>2</sub> O <sub>3</sub>	300	98	10% CO	98	250–300	12,000	[35]
CoOx/ $\gamma$ -Al <sub>2</sub> O <sub>3</sub>	300	0	10% CO	100	250–300	12,000	[35]
CuO-CoOx/ $\gamma$ -Al <sub>2</sub> O <sub>3</sub>	300	100	10% CO	100	250–300	12,000	[35]
CuCeAl/ $\gamma$ -Al <sub>2</sub> O <sub>3</sub>	400	100	10% CO	100	300–400	24,000	[34]
CuAl/ $\gamma$ -Al <sub>2</sub> O <sub>3</sub>	400	20	10% CO	85	300–400	24,000	[34]
CeAl/ $\gamma$ -Al <sub>2</sub> O <sub>3</sub>	400	6	10% CO	50	300–400	24,000	[34]
Ni/TiO <sub>2</sub>	200	60	1% CO		50–200	50,000	[37]
Cu/TiO <sub>2</sub>	200	50	1% CO		50–200	50,000	[37]
Cr/TiO <sub>2</sub>	200	31	1% CO		50–200	50,000	[37]
Fe/TiO <sub>2</sub>	200	29	1% CO		50–200	50,000	[37]
Mn/TiO <sub>2</sub>	200	95	1% CO		50–200	50,000	[37]
Cu <sub>2</sub> Co <sub>9</sub> CeO <sub>x</sub>	250	100	2%CO		250–400	20000	[53]
In/TiO <sub>2</sub> / $\gamma$ -Al <sub>2</sub> O <sub>3</sub>	600	45	2.1%CO	45	400–600	7000	[27]
Ag/TiO <sub>2</sub> / $\gamma$ -Al <sub>2</sub> O <sub>3</sub>	600	43	2.1%CO	43	400–600	7000	[27]
InAg/ $\gamma$ -Al <sub>2</sub> O <sub>3</sub>	600	46	2.1%CO	46	400–600	7000	[27]
InAg/TiO <sub>2</sub> / $\gamma$ -Al <sub>2</sub> O <sub>3</sub>	600	68	2.1%CO	68	400–600	7000	[27]
CeZr/La <sub>2</sub> O <sub>3</sub> -Al <sub>2</sub> O <sub>3</sub>	700	80	CO/NO = 1:1	55	500–700	2868	[30]
0.5Pd/CeZr/La <sub>2</sub> O <sub>3</sub> -Al <sub>2</sub> O <sub>3</sub>	300	100	CO/NO = 1:1	25	250–700	2868	[30]
1.5Pd/CeZr/La <sub>2</sub> O <sub>3</sub> -Al <sub>2</sub> O <sub>3</sub>	300	100	CO/NO = 1:1	30	250–700	2868	[30]

### 2.3. Reaction Mechanism

Numerous works have been conducted to explore the mechanism of NO removal by Co with different catalysts. Since different catalysts exhibit different unique reaction mechanisms of NO removal, the present paper focuses on those of interest, which are the reactions of NO removal by CO on Ni/CeO<sub>2</sub>, AO<sub>x</sub>/CuO<sub>y</sub>/MOF (A = Fe, Ni, Co, Mn), and Cr-Cu/CeO<sub>2</sub> catalysts. Their reaction mechanisms are summarized in Figure 3a–c.

The active center of the catalyst and the process of NO removal by CO have been studied. There are two types of nitrogen oxides adsorbed on the catalyst: NO or NO<sub>x</sub> (x = 2 or 3). As shown in Figure 3a, during NO adsorption, NO does not dissociate on the oxidized surface of NiO/CeO<sub>2</sub> to produce nitrogen atoms. When two NO molecules are near the Ce<sup>3+</sup> oxygen vacancy, nitrite will be formed, and the decomposition of nitrite leads to the formation of N<sub>2</sub>O. As the surface oxygen occupies the active site, the formation of N<sub>2</sub>O decreases gradually. These nitrite species are important intermediates for the formation of N<sub>2</sub>, NO, N<sub>2</sub>O, etc. [55]. Yao et al. [56] found that on the Ce<sub>x</sub>Sn<sub>1-x</sub>O<sub>2</sub> catalyst, NO molecules are preferentially adsorbed on the catalyst surface due to its unpaired electrons. Those NO molecules generate a variety of nitrite and nitrate species, thus further inhibiting the adsorption of CO species. However, the contact between CO molecules and the surface of Ce<sub>x</sub>Sn<sub>1-x</sub>O<sub>2</sub> catalyst will lead to the reduction of catalyst during the heating process, thus forming more surface Ce<sup>3+</sup> and oxygen vacancy. CO species adsorbed on the surface Ce<sup>3+</sup> can react with O radical generated by the decomposition of NO on the adjacent oxygen vacancy to generate CO<sub>2</sub>. The remaining N radical can combine with NO molecules to form N<sub>2</sub>O, or their own combination to produce N<sub>2</sub>.

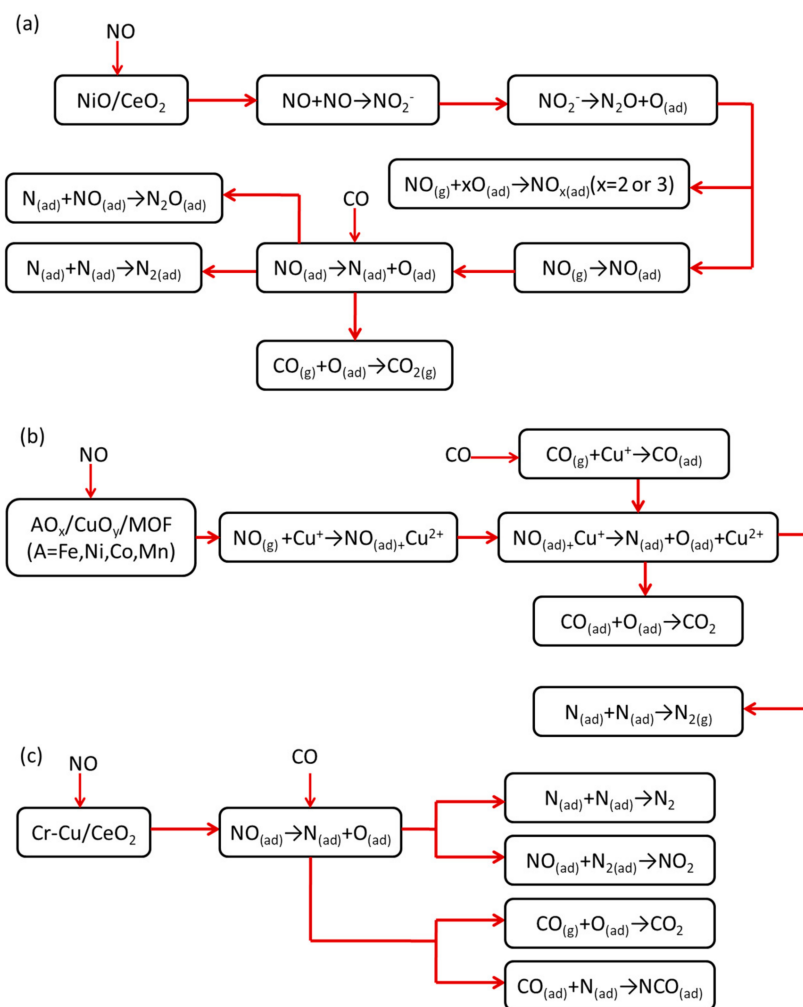


**Figure 3.** Schematic illustration of possible NO+CO reaction mechanism over (a) Ni/CeO<sub>2</sub>, (b) AO<sub>x</sub>/CuO<sub>y</sub>/MOF (A = Fe, Ni, Co, Mn), and (c) Cr-Cu/CeO<sub>2</sub> catalysts.

Molecular adsorption is a key step in the gas–solid phase reaction. The adsorption site provided by the catalyst plays an important role in the catalytic reaction. For non-precious metal catalysts, the active center includes both active metal ions and oxygen vacancies. The key to efficient NO removal relies on the amount of surface oxygen vacancies, the degree of dispersion of the metal oxide, and the redox capability of the catalyst. Zou et al. [57] synthesized Cu<sub>2</sub>O rhombohedral dodecahedron (110), octahedron (111), and cube (100). The TPR results showed that the order of reduction ability is (110) > (111) > (100). The order of activity of the reaction is consistent with its order of reducing ability. Metal Cu nanoparticles formed by the exposed crystal faces of Cu<sub>2</sub>O are observed on the surface. NO adsorption/dissociation is one of key steps, and the crystal plane effect has an important influence on catalytic behavior and in-situ structural transformation. An increase in surface oxygen vacancies can promote the reaction of NO removal by CO. The CO and NO adsorbed on the carrier undergo a “hydrogen drop” reaction with the hydroxyl group to form NH<sub>3</sub>, and water-induced hydroxylation promotes the formation of NH<sub>3</sub> [57]. As shown in Figure 3b, Qin et al. [49] investigated AO<sub>x</sub>/CuO<sub>y</sub>/MOF (A = Fe, Ni, Co, Mn) catalyst, and found that the addition of A can improve the catalytic efficiency. In the organic framework, NO(g)+Cu<sup>+</sup> → NO(ad)+Cu<sup>2+</sup>, the adsorbed CO species reacts with O radicals to form CO<sub>2</sub>, and the N radical and another N radical generate N<sub>2</sub>. The Co-O surface is active for CO adsorption, and CO can absorb lattice oxygen from the cobalt spinel oxide to form CO<sub>2</sub>. The adsorbed NO molecules desorb off the dissociation to form N<sub>2</sub>, thereby regenerating the surface active sites of CO and NO adsorption. Since

$\text{Rh}^{3+}$  can occupy the octahedral position in the  $\text{Co}_3\text{O}_4$  spinel, its substitution enhances the reduction process of  $\text{CO}_2$  from surface desorption and enhances the chemical adsorption capacity of NO.  $\text{Pd}^{2+}$  and  $\text{Ru}^{4+}$  cations occupy the tetrahedral position of cobalt spinel oxide, which has a lower effect on NO conversion than  $\text{Rh}^{3+}$  [12].

Regarding the formation of oxygen vacancies, Wang et al. [55] proposed a model of NO+CO interaction, including the following three steps: reducing the surface of the catalyst by CO, generating oxygen vacancies, and dissociating the adsorbed NO in the vacancies scavenging of surface O free radicals by CO, avoiding the inhibition of oxygen accumulation with the regeneration of surface oxygen vacancy. On the CuNCoA catalyst, oxygen vacancies can weaken the NAO bond to promote dissociation of NO. The addition of oxygen reduces the NO conversion, because  $\text{O}_2$  produces O radicals and reacts with the adsorbed CO to form  $\text{CO}_2$  [35]. Deng et al. [58] found that the contact of CO with the Cu/TC-60:1 catalyst resulted in the catalyst being reduced to  $\text{Ti}^{3+}$  and  $\text{Ce}^{3+}$  and producing more surface oxygen vacancies. During heating,  $\text{Cu}^{2+}$  can be reduced to  $\text{Cu}^+$ . As a result, more CO adsorption sites are generated due to the presence of more  $\text{Cu}^+$ . In addition,  $\text{Cu}^{2+}$  is further reduced to CuO metal,  $\text{N}_2\text{O}$  is further reduced to  $\text{N}_2$  and O at high temperature, and adjacent CO and O combine to form  $\text{CO}_2$ , and new active sites on the surface are regenerated. NO is decomposed and adsorbed on the surface of the catalyst, and the obtained O immediately forms an oxygen balance with the surface of Cr-Cu/ $\text{CeO}_2$  and reacts with CO adsorbed at the  $\text{Cu}^+$  site to form  $\text{CO}_2$ . CO adsorption to  $\text{Cu}^+$  and NO adsorption is a key step [39], as shown in Figure 3c.

In presence of oxygen, the NO-CO reaction will not happen until the oxygen concentration is below a threshold value due to the stronger adsorption ability of oxygen than NO [19]. The reduction of NO by CO is promoted by the increase of CO concentration, but it is limited by the increase of oxygen concentration. Thus, in our point of view, NO reduction is dominated by NO adsorption and decomposition on the active site of the catalyst [20].

### 3. Catalysts for NO Removal by $\text{CH}_4$

Compared with other hydrocarbons, methane is cheaper and relatively easier to be obtained. Methane is the simplest molecule in hydrocarbon molecules, and its structure is highly symmetrical and inert. It is difficult to absorb methane molecules on the catalyst surface, which hinders the reaction of  $\text{NO}_x$  reduction [17].

Catalysts for the reaction of  $\text{NO}_x$  reduction by  $\text{CH}_4$  can also be divided into two categories: non-precious metal and precious metal series catalysts. Precious metal catalysts (Pt, Pd, etc.) have high activity; their temperature range, however, is narrow. Once occurring deactivation, it is hard to regenerate. In contrast, non-precious metal catalysts are often cheaper, but their activity is limited. Table 2 shows some of catalysts for catalytic reduction of  $\text{NO}_x$  reduction by  $\text{CH}_4$  under different conditions.

#### 3.1. Precious Metal Catalyst

The activity of the precious metal catalyst of  $\text{CH}_4$ -SCR is essentially impacted by the active component and its support. The active component is the key material for the catalyst to exhibit activity, while the primary role of the carrier is to increase the surface area of the catalyst, providing a "location" for the active component and enhancing sufficient mechanical strength and thermal stability of the catalyst.

A  $\text{Pt}_{(0.5\%<x<4\%)}\text{H}_{(0.95)}$  ALMCM-41 catalyst with different platinum contents was prepared by Sakmeche et al. [59]. The activity test results showed that the NO conversion rate is the highest at  $\text{CH}_4/\text{O}_2 = 2$ , and the highest activity of the catalyst occurs at  $x = 2.5$  wt.%. Once the reaction temperature exceeds  $400^\circ\text{C}$ , the activity of the catalyst decreases, because the excessive temperature may destroy the structure of the catalyst, resulting in a large reduction in the active site. On the Pd/H-MOR catalyst, Pd exists in the form of  $\text{Pd}^{2+}$ , which is responsible for the high catalytic activity of NO removal by  $\text{CH}_4$  in the presence of oxygen. The acid sites of the carrier are important to the NO removal. The zirconia

was sulfated to obtain Pd/Co-SZ. Compared with Pd/Co-HMOR, the NO conversion rate is lower than that of the latter, indicating that the acidity of the carrier is beneficial to the improvement of catalytic activity [60]. In the experiment of catalytic reduction of NO by methane in 0.1 wt.% Pd/sulfated alumina (SA) catalyst, Pd supported on  $\text{Al}_2\text{O}_3$  mainly exists as oxide, while Pd supported on SA exists mainly in isolated  $\text{Pd}^{2+}$  ion. Thus, sulfation can promote the reduction reaction [61]. Azambre et al. [62] prepared Pd sulfated ceria–zirconia (SCZ) catalysts by impregnation of a  $\text{PdCl}_2$  precursor dissolved in ammonia solution on a sulfated  $\text{Ce}_{0.21}\text{Zr}_{0.79}\text{O}_2$  support for the SCR of NO by methane under the conditions 150 ppm NO; 1500 ppm  $\text{CH}_4$ ; 7 vol.%  $\text{O}_2$ ; catalyst with Pd loadings in the range 0.24–0.53 wt.% best achieved  $\text{CH}_4$ -SCR performances with 30–35% NO conversion to  $\text{N}_2$  around 350–400 °C.

Indium is also a relatively common metal in the experiment of NO removal by  $\text{CH}_4$ . Hernán et al. [63] studied the characteristics of species produced by continuous exchange of indium and palladium in H-mordenite (HM). Pd was added to the In/HM catalyst by reduction solid-state ion exchange, and the catalytic effect was dependent on the In loading of the sample. For higher loadings of PdIn/HM, the addition of Pd results in an increase in catalytic activity. The activity of the catalyst is closely related to the nature of the supported metal and the amount of loading. In order to study the relationship between the structure of indium sites and their catalytic properties, Sowade et al. [64] prepared In/ZSM-5 catalysts in different ways (water ion exchange at different pH values, solid state ion exchange, sublimation and transmission reaction with  $\text{InCl}_3$  indium source). The indium oxide was found to be the active site, and the reaction of NO removal by  $\text{CH}_4$  on In/ZSM-5 required an acidic site. Mixing the two carriers together in a certain ratio is also one of the commonly used means for increasing the activity of the catalyst. It was found that the activity of the In/ $\text{WO}_3/\text{ZrO}_2$  catalyst is significantly higher than that of  $\text{WO}_3/\text{ZrO}_2$ ,  $\text{ZrO}_2$ , and In/ $\text{ZrO}_2$ . The characterization results showed that indium has two forms of  $\text{InO}^+$  and  $\text{In}_2\text{O}_3$ , and only  $\text{InO}^+$  is active for the reaction of methane to reduce NO [65]. The synthesis conditions, such as ion exchange liquid concentration and calcination temperature, have significant effects on the catalytic activity of  $\text{CH}_4$  selective catalytic reduction of  $\text{NO}_x$  [66]. Experiments have shown that when the exchange liquid concentration is 0.033 M and the calcination temperature is 500 °C, the In/H-Beta catalyst exhibits excellent activity; its  $\text{NO}_x$  removal rate can reach 97.6%.

The noble metal-containing zeolite-based catalysts have good activity in NO reduction by  $\text{CH}_4$ . Their activity highly depends on the noble metal loaded content, and a peak activity occurs at a certain content, because excessive metal loading could block the pores of the catalyst. Synergistic effects may happen when a non-noble metal is doped on the precious metal catalyst, thereby increasing the reaction efficiency of the catalyst. Azizi et al. [67] prepared a series of Ag/ $\gamma\text{-Al}_2\text{O}_3$  catalysts with different Ag loadings (2–8 wt.%). The results showed that the activity of the catalyst is the highest when the loading of silver is 2 wt.%. Comparison of  $\text{Pd}_x/\text{HMOR}$  ( $x = 0.15, 0.3, 0.5, 0.7$ ),  $\text{Pd}_{0.3}\text{Ce}_y/\text{HMOR}$  ( $y = 1, 2, 3, 5, 10$ ),  $\text{Ce}_2/\text{HMOR}$  catalyst, and  $\text{Pd}_{0.3}\text{Ce}_2/\text{HMOR}$  showed the highest catalytic activity in NO reduction by  $\text{CH}_4$ . The characterization results showed that the addition of Ce to the Pd/HMOR catalyst can improve the catalytic performance [68]. Sun et al. [69] used the impregnation method to prepare  $\text{Ag}_{(x)}/\text{ZSM-5}$  ( $x = 3, 6, 9$ ) catalyst. The study showed that the acidity and acid amount of catalyst changes when Ag is loaded on ZSM-5 molecular sieve, and the N adsorption and NO removal performance of catalyst is improved. At the same time, with the increase of Ag load, larger Ag grains are observed, which is conducive to catalyst activation and enhanced NO removal performance. Rodrigues et al. [70] doped palladium and cobalt into zeolite by two-step post-synthesis method to prepare  $\text{Pd}_{0.15}\text{SiBEA}$  and  $\text{Co}_x\text{Pd}_{0.15}\text{SiBEA}$  zeolites (where  $x = 1.0$  and 3.0 wt.% Co). These techniques allow the cobalt to be present as isolated mononuclear Co(II) species in both  $\text{Co}_{1.0}\text{Pd}_{0.15}\text{SiBEA}$  and  $\text{Co}_{3.0}\text{Pd}_{0.15}\text{SiBEA}$  catalysts. The catalytic activity of  $\text{Co}_x\text{Pd}_{0.15}\text{SiBEA}$  strongly depends on the content of this particular Co(II) species. When Co content increase from 1.0 to 3.0 wt.%, the NO conversion in the  $\text{CH}_4$ -SCR process increases from maximum value of 25% to 55%.

The methane conversion is lower than 15% for  $\text{Co}_{1.0}\text{Pd}_{0.15}\text{SiBEA}$  at 230–460 °C, but for  $\text{Co}_{3.0}\text{Pd}_{0.15}\text{SiBEA}$  is much higher at 400–500 °C, reaching maximum value of 35% at 500 °C.

The reaction of NO removal by  $\text{CH}_4$  often involves multiple bond cracking and reforming, thus requiring multiple active centers. It is rare for a single active component to have these catalytic centers at the same time. Multiple active components catalyst is more often encountered in practice. Therefore, doping different elements together to obtain a highly active catalyst is of great interest. In the Pd/H-MOR and Ce-Pd/H-MOR catalysts, Ce added to the Pd/H-MOR catalyst increases the activity of  $\text{CH}_4$  to NO removal [71]. Mendes et al. [7] prepared  $\text{Pd}_{0.3}\text{Ce}_2/\text{HBEA}$  catalyst and  $\text{Pd}_{0.3}\text{Ce}_2/\text{HMOR}$  catalyst by ion exchange method. The catalyst was tested in a dual bed configuration, where  $\text{Pd}_{0.3}\text{Ce}_2/\text{HBEA}$  is placed on the first layer and  $\text{Pd}_{0.3}\text{Ce}_2/\text{HMOR}$  is placed on the second layer. The experimental results showed that the placement in the above manner can significantly improve the catalytic performance. Both catalysts exhibited synergistic effects compared to a single catalyst. Better and more uniform dispersion greatly improves its catalytic performance for  $\text{NO}_x$  reduction [72]. In the Pt/La- $\text{Al}_2\text{O}_3$  and Pt/ $\text{Ce}_{0.67}\text{Zr}_{0.33}\text{O}_2$  monolith catalysts, the latter has higher activity [73].

### 3.2. Non-Precious Metal Catalyst

#### 3.2.1. Transitional Metal Catalysts

The transition metals Fe, Co, Ni, Al, and Cu are commonly non-precious metal active ingredients. In the Cu-based catalyst system with high surface area structure, the copper species exists in the form of massive CuO crystals, which can lower the temperature of the NO desorption peak [74]. The methane combustion reaction that may occur in the  $\text{CH}_4$  reduction of NO reduces the activity of the catalyst [17]. The addition of  $\text{O}_2$  inhibits the removal of NO, but promotes the conversion of  $\text{CH}_4$ . Ren et al. [75] prepared Fe/ZSM-5 catalysts with different Fe loadings by the impregnation method. The results showed that the activity of this series of catalysts is very poor [76]. MOR is a zeolite molecular sieve with uniform micropores. The pore size is comparable to the general molecular size, with a unique regular crystal structure and a strong acid center. Among the Co- and Ni-exchanged Na-MOR (Si/Al = 9.2) catalysts prepared by ion exchange, Co-MOR and Ni-MOR are active for the NO removal by  $\text{CH}_4$ . Co-MOR has a high catalytic ability for the decomposition of  $\text{N}_2\text{O}$  [77]. Hong et al. [78] prepared  $\text{Co}_x$ -MOR catalysts with different Co contents by the impregnation method. The performance test results showed that the cobalt loading is closely linked to the catalytic ability of Co-MOR. When the loading of Co is 10 wt.%, the  $\text{Co}_{10}$ -MOR catalyst exhibits a high catalytic activity in the reaction of NO removal by  $\text{CH}_4$ . The experiment showed that the carrier, the concentration of the ion exchange liquid, and the calcination temperature also affect the activity of the catalyst. Li [14] found that adding  $\text{Co}_3\text{O}_4$  to the In/H-Beta catalyst can effectively improve the water resistance and sulfur resistance of catalyst. This is because the  $\text{Co}_3\text{O}_4$  has good oxidation resistance to enhance the catalyst and  $\text{CH}_4$  adsorption effect. It also makes the  $\text{CH}_4$  more likely to be activated. Janas et al. [79] prepared FeAlBEA and FeSiBEA zeolites by a conventional ion exchange and a two-step post-synthesis method, respectively. Results show the catalytic activity of FeAlBEA and FeSiBEA catalysts in SCR of NO with ethanol or methane depends on the nature of Fe species and the presence of Al and Fe ions in the zeolite framework.  $\text{Fe}_{1.4}\text{AlBEA}$  has higher activity in the SCR of NO with methane and much higher selectivity toward  $\text{N}_2$  than  $\text{Fe}_{1.3}\text{SiBEA}$  catalyst because of its higher strength and amount of Brønsted and Lewis acidic centers.

#### 3.2.2. Effect of Reaction Conditions

The reaction conditions will also affect the selective catalytic reduction of NO by  $\text{CH}_4$ . Charrad et al. [80] prepared Co/H-SSZ-13 catalyst and investigated effects of the reaction conditions. The experimental results showed that when 500 ppm NO, 1.8%  $\text{CH}_4$ , 3.7%  $\text{O}_2$ , and 5.5%  $\text{H}_2\text{O}$  were supplied in, while the GHSV during the control reaction was kept at  $15,000 \text{ h}^{-1}$ , the nearly 100% NO conversion rate can be obtained.

**Table 2.** Catalysts for catalytic reduction of NO<sub>x</sub> by CH<sub>4</sub> under different conditions.

Catalyst	Maximum Conversion Temperature/°C	NO Conversion Rate/%	Reducing Agent	O <sub>2</sub> /%	N <sub>2</sub> Selectivity/%	Active Temperature Window/°C	GHSV /h <sup>-1</sup>	References
Pd/Co-HMOR	500	42	4000 ppm	10		450–550	60,000	[60]
Pd/Co-SZ	550	37	4000 ppm	10		450–550	60,000	[60]
Co <sub>1.0</sub> Pd <sub>0.15</sub> SiBEA	420	26	1500 ppmCH <sub>4</sub>	7		400–450	40,000	[70]
Co <sub>3.0</sub> Pd <sub>0.15</sub> SiBEA	480	56	1500 ppmCH <sub>4</sub>	7		400–500	40,000	[70]
Pd <sub>0.24</sub> /SCZ28	400	31	1500 ppmCH <sub>4</sub>	7		350–450	40,000	[62]
Pd <sub>0.47</sub> /SCZ28	400	34.5	1500 ppmCH <sub>4</sub>	7		350–450	40,000	[62]
Pd <sub>0.53</sub> /SCZ28	400	33.6	1000 ppmCH <sub>4</sub>	7		350–450	40,000	[62]
Pd <sub>0.99</sub> /SCZ28	385	17	1000 ppmCH <sub>4</sub>	7		350–450	40,000	[62]
Pd <sub>1.04</sub> /SCZ28	300	7	1000 ppmCH <sub>4</sub>	7		300–350	40,000	[62]
Fe <sub>1.3</sub> Si/BEA	350	18	2000 ppmCH <sub>4</sub>	2	85	300–400	40,000	[79]
Fe <sub>1.4</sub> Al/BEA	400	30	2000 ppmCH <sub>4</sub>	2	95	300–500	40,000	[79]
Pt/La-Al <sub>2</sub> O <sub>3</sub>	600	100	2000 ppmCH <sub>4</sub>	0.5		500–600	40,000	[73]
Pt/Ce <sub>0.67</sub> Zr <sub>0.33</sub> O <sub>2</sub>	450	100	2000 ppmCH <sub>4</sub>	0.5		450–600	40,000	[73]
In/H-BEA	552	98	600 ppmCH <sub>4</sub>	5		450–550	20,000	[8]

### 3.2.3. Effect of Carrier

Zeolite is a common carrier for the catalyst preparation. Lim et al. [81] prepared four cage-type small pore zeolites with different framework topologies, namely Co-CHA, Co-RTH, Co-UF1, and Co-LTA with 10–11 and 0.44–0.49 Si/Al and Co/Al ratios, respectively. The structure of cobalt ion is shown in Figure 4. Experiments have found that the catalyst has a high NO conversion rate as high as 90% in a humid environment of 500 °C and a carrier silicon-to-aluminum ratio of 6. The CH<sub>4</sub>-SCR activity of all four catalysts decreases in wet conditions, and the activity of Co-CHA is least influenced by water vapor. The characterization results show that the framework topology and composition of the zeolite support are the key factors that determine the position of Co<sup>2+</sup> ions in the zeolite and the catalyst activity.

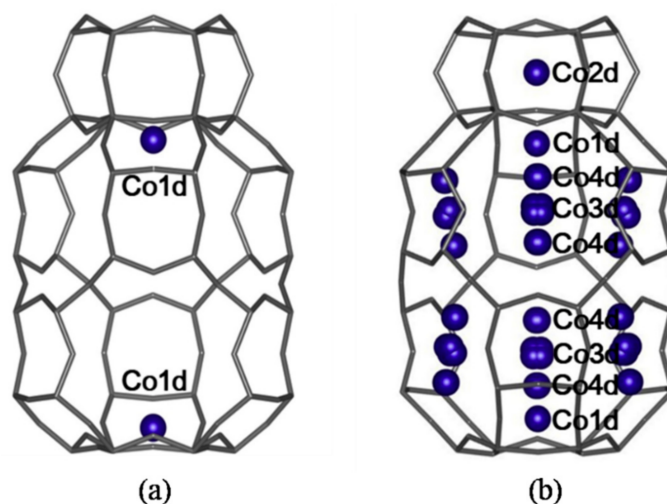


**Figure 4.** Structure of cobalt ion in zeolite: (a) Co-CHA-6.0-0.39/Co-CHA-10-0.46/Co-CHA-16-0.47 (b) Co-CHA-2.4-0.40. Color code: Si and O, grey; Co, blue. [81].

### 3.2.4. Effect of Pore Size and Structure

Conventional mesoporous or macroporous Al<sub>2</sub>O<sub>3</sub> catalysts have a low specific surface area and a wide pore size distribution, which limits their practical application. In a supported catalyst, the difference in the amount of active component supported affects the activity of the catalyst. Li et al. [82] chose AEO-7 as a soft template and prepared ultra-microporous nanocrystalline Cu/Al<sub>2</sub>O<sub>3</sub> (pore size 1–2 nm) by evaporation-induced self-assembly (EISA). After removing the template at 500 °C, the catalyst shows a high

specific surface area. The pore volume is large enough to allow diffusion of the reactants and product surfaces. The stencil effect of the surfactant is the key to obtaining a high surface area material. It was found that the ultramicroporous nanocrystalline Cu/Al<sub>2</sub>O<sub>3</sub> catalyst has a narrow pore size distribution, high thermal stability, large surface area, and good dispersibility of active copper. Therefore, the activity of the ultramicroporous Cu/Al<sub>2</sub>O<sub>3</sub> catalyst is significantly higher than that of the conventional Cu/Al<sub>2</sub>O<sub>3</sub> catalyst.

### 3.2.5. Non-Precious Multi-Metal/Metal Oxide Catalyst

Introducing new experimental means or modifying the catalyst could increase the efficiency of the CH<sub>4</sub> reduction NO reaction. Li et al. [83] found that among the Mn/ZrO<sub>2</sub>, Mn/Na<sub>2</sub>SO<sub>4</sub>/ZrO<sub>2</sub>, and Mn/SZ (sulfation) catalysts, the third catalyst has the highest activity. The characterization results showed that the strong Brønsted and Lewis acid sites in the Mn/SZ catalyst are essential for the methane reduction of NO. Metal modification of conventional catalysts is one of the effective methods to improve the activity and water resistance of catalyst. Lin et al. [13] used Fe to modify the Al<sub>2</sub>O<sub>3</sub> supported Ga<sub>2</sub>O<sub>3</sub> catalyst. They prepared xFe/Ga<sub>2</sub>O<sub>3</sub>-Al<sub>2</sub>O<sub>3</sub> catalyst by precipitation method. The test results showed that the Fe modified catalyst has better activity and water resistance at high temperature. Chou et al. [84] studied the effects of active component copper content, auxiliary component (Mg, Pr, Co, Y, La), and their contents on the NO removal performance of catalyst. They found that the optimal content of active component copper is 5 wt.%. The best auxiliary agent is Co, and the optimal content is 5 wt.%. The optimal catalyst 5Cu-5Co/γ-Al<sub>2</sub>O<sub>3</sub> showed good hydrothermal stability and the ability to adapt to air speed changes at 500 °C, and the catalyst in the oxygen atmosphere is conducive to the catalytic reaction of NO removal.

### 3.3. Reaction Mechanism

In this paper, three representative NO removal by CH<sub>4</sub> processes are discussed, and the reaction mechanisms of NO removal by CH<sub>4</sub> process with Co/H-ZSM, In/WO<sub>3</sub>/ZrO<sub>2</sub>, and In/H-BEA catalysts are summarized as shown in Figure 5.

The researchers explored the reaction process of reducing NO by CH<sub>4</sub> through extensive experimental works. Figure 5a describe a reaction scheme for NO removal by CH<sub>4</sub> over Co/H-ZSM catalyst. In the Co/H-ZSM catalyst, the reaction of NO oxidation to NO<sub>2</sub> is accelerated at the acid sites of the Brønsted acid. The reaction of NO-CO provides an intermediate product for the reaction of CH<sub>4</sub>-NO. Surface nitrate species react with methane to produce an active intermediate for the CH<sub>4</sub>-NO reaction. The activation of the C-H bond in CH<sub>4</sub> serves as a rate determining step for the NO removal reaction [17]. It was found that the formation of NO is significantly increased when high concentration of steam is introduced in the enriched condition, which is due to the increase of OH roots caused by the addition of high concentration of steam in the enriched condition [85]. The adsorbed nitrate species and HCOO<sup>-</sup> have been shown to be key intermediates for the CH<sub>4</sub>-NO reaction in the presence of O<sub>2</sub>.

When NO cannot be directly adsorbed on the surface of the catalyst to form nitrate species, the oxidation of NO to NO<sub>2</sub> is the only way to form nitrate [86]. A simplified reaction mode for the NO removal by CH<sub>4</sub> over In/WO<sub>3</sub>/ZrO<sub>2</sub> catalysts is presented in Figure 5b. On In/WO<sub>3</sub>/ZrO<sub>2</sub> (In/WZr) catalyst, NO is firstly oxidized by O<sub>2</sub> to NO<sub>2</sub>. The adsorbed NO<sub>2</sub> then form nitrate species, which are adsorbed on two different sites. One is adsorbed on the WZr carrier and the other is adsorbed on the InO<sup>+</sup> site. At low temperatures, active sites for CH<sub>4</sub> activation are covered by nitrate species, which hinders the CH<sub>4</sub>-NO reaction. As the temperature increases, nitrate species adsorbed on the WZr carrier disappear and the active sites are restored to maintain the CH<sub>4</sub> activation and CH<sub>4</sub>-NO reaction at 350 °C. The formation of HCOO<sup>-</sup>, one key intermediate for NO removal by CH<sub>4</sub>, is associated to the uncovered WZr carrier and the NO<sub>3</sub><sup>-</sup> species adsorbed on the InO<sup>+</sup> site. The WZr carrier promotes CH<sub>4</sub> decomposition and the NO<sub>3</sub><sup>-</sup>

species adsorbed on  $\text{InO}^+$  provides active oxygen. The  $\text{N}_2$  is formed in the interaction between the intermediates of  $\text{HCOO}^-$  and nitrate species.

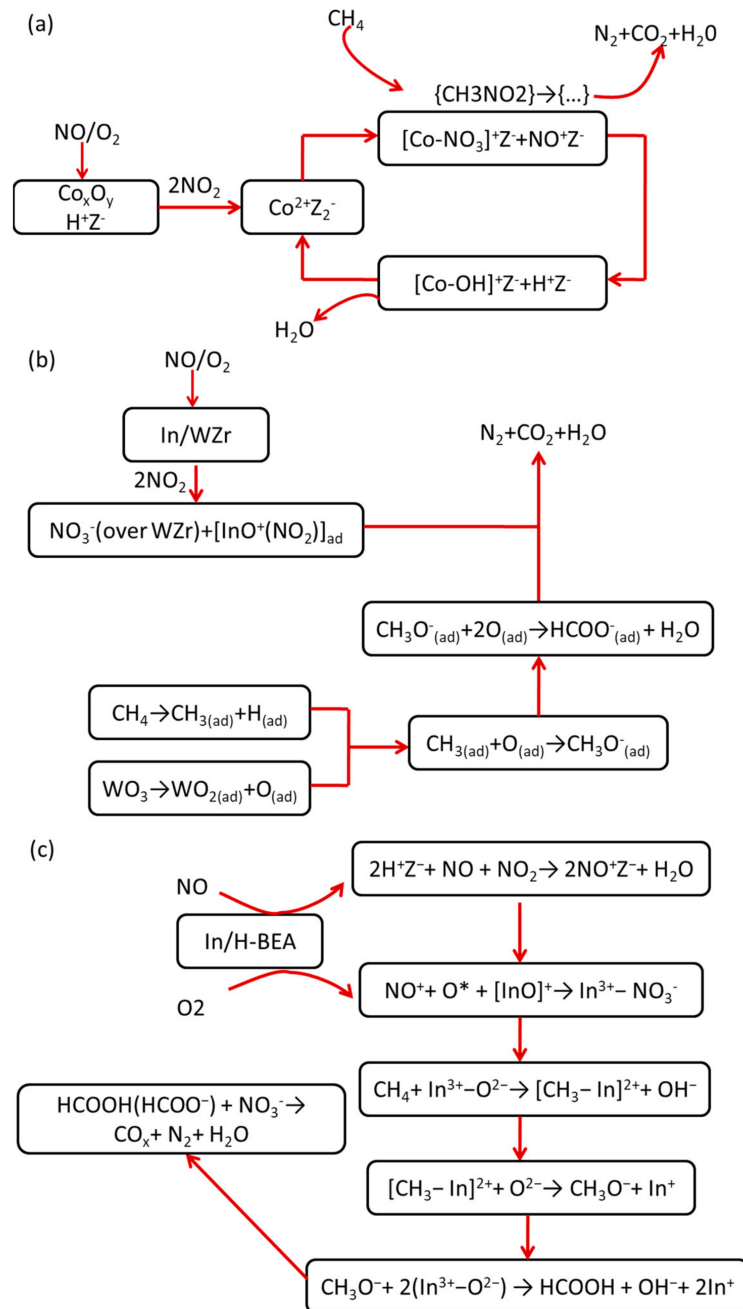


**Figure 5.** Schematic illustration of possible  $\text{NO} + \text{CH}_4$  reaction mechanism over (a)  $\text{Co}/\text{H-ZSM}$ , (b)  $\text{In}/\text{WO}_3/\text{ZrO}_2$ , and (c)  $\text{In}/\text{H-BEA}$  catalysts.

Figure 5c indicates the process of  $\text{NO}$  removal by  $\text{CH}_4$  over  $\text{In}/\text{H-BEA}$  catalysts. Pan et al. [8] found that  $\text{NO}$  and  $\text{O}_2$  adsorbed on the Brønsted acid sites of the molecular sieve to produce  $\text{NO}^+$ . Subsequently, on the  $\text{InO}^+$  active site  $\text{NO}^+$  forms important intermediates of nitrates. Methane then was activated to generate  $-\text{CHO}$  and  $-\text{COOH}$ , etc., carbonaceous species. Finally, on the  $\text{InO}^+$  active site, the nitrate reacts with the carbonaceous material to form  $\text{N}_2$ ,  $\text{H}_2\text{O}$ , and  $\text{CO}_2$ .

In terms of oxygen in the  $\text{NO}$  removal by  $\text{CH}_4$ , the inhibition of oxygen is different from that of  $\text{CO}-\text{NO}$  reaction; oxygen has a dual effect on the  $\text{NO}$  removal by methane. In the process of  $\text{NO}$  oxidation to  $\text{NO}_2$  and  $\text{NO}$  adsorption, the higher the oxygen content,

the faster the process rate. In the methane oxidation process, the higher the oxygen content, the lower the catalytic efficiency. In the experiment of catalytic reduction of NO by methane, NO is first oxidized to NO<sub>2</sub>, and then NO<sub>2</sub> oxidizes hydrocarbons to C<sub>x</sub>H<sub>y</sub>O<sub>z</sub> intermediate, which is the actual reducing agent responsible for regenerating the active sites involved in the direct decomposition of NO-N<sub>2</sub> [7]. In addition, the negative effect of oxygen on NO removal efficiency stems from the competitive reaction of oxygen and NO with respect to CH<sub>4</sub>, and the oxygen in the flue gas is an essential factor for the oxidation of NO to the catalyst surface. Oxygen plays a dual role of positive (promoting adsorption) and negative (suppressing reduction) in the NO reaction process. Therefore, a suitable catalyst should be selected to react methane with NO to increase the conversion rate of NO. To our knowledge, the technology of NO removal by CH<sub>4</sub> has not been widely applied in industrial equipment due to its catalytic activity, high requirements on reaction flue gas atmosphere, and narrow temperature window.

#### 4. Catalysts for NO Removal by H<sub>2</sub>

Compared with the traditional NH<sub>3</sub>-SCR, selective catalytic reduction of NO with H<sub>2</sub> (H<sub>2</sub>-SCR) in the presence of O<sub>2</sub> has attracted much attention, because of the advantage of introducing no secondary pollutants and without other disadvantages such as ammonia slip and catalyst deactivation. Meanwhile, H<sub>2</sub>-SCR can remove NO<sub>x</sub> at lower reaction temperature (<200 °C).

At present, the reports on NO<sub>x</sub> reduction by H<sub>2</sub> are mainly concentrated on noble metal catalysts, while very limited works have been conducted on non-precious metal catalysts. Therefore, we will focus on the research progress of precious metal catalysts in recent years from the traditional carrier and new carrier. Some of catalysts for catalytic reduction of NO<sub>x</sub> by H<sub>2</sub> under different conditions are tabulated in Table 3.

##### 4.1. Traditional Carrier

Traditional carriers of catalyst for NO reduction include metal oxide (e.g., Al<sub>2</sub>O<sub>3</sub> [87], SiO<sub>2</sub> [88]), zeolite (ZSM-5 [89], ZIF [90], H-Zeolite Y (HY) [91]), aluminate spinel [92], and perovskite-type composite oxide [93]. They are relative stable and commonly compatible with most of precious and non-precious metals. Most of them do not have or have very limited catalytic ability, except zeolite carrier. NO reduction performance of catalysts made from the traditional carrier is affected by synthesis condition, doped metal, and carrier's structure and acidity, etc.

The acidity of carrier strongly affects the dispersion and chemical state of Pt. Li et al. [87] reported that among the Pt/MgO, Pt/γ-Al<sub>2</sub>O<sub>3</sub>, Pt/ZrO<sub>2</sub>, and Pt/HZSM-5 catalysts, the catalyst activity is significantly different. On the representative acidic carrier of HZSM-5, Pt mainly exists in the form of metal. This causes the supported platinum catalyst to have very low activity at low temperatures before the reduction treatment. At this time, the acidity of HZSM-5 will also influence the reduction of NO<sub>x</sub> adsorption on the catalyst surface. Yu et al. [94] explored the catalytic performances of platinum catalysts supported on ZSM-5, ZSM-35, and Beta for the selective catalytic reduction of NO by hydrogen. 1%Pt/ZSM-35 reaches the best activity with a maximum NO conversion of 80.8% and N<sub>2</sub> selectivity of 68.5% at 120 °C with GHSV = 80,000/h space velocity. NH<sub>4</sub><sup>+</sup> is found to be the key intermediate in H<sub>2</sub>-SCR. As Pt loading exceeds 1.0 wt.% catalyst, an activity declines, because a loss of strong acid sites is observed. Later, they [95] doped Cr on Pt/ZSM-35 and tested its performance in H<sub>2</sub>-SCR process, and they got an attractive increase of NO conversion from 80.5% to 94.7% at 120 °C on Pt-Cr/ZSM-35 catalyst. Challagulla et al. [90] produced a Pt/ZIF-8 catalyst with a perfect body-centered cubic structure. As shown in Figure 6, FE-SEM and HR-TEM images show that metal platinum nanoparticles are synthesized with high surface area porous ZIF-8 and original ZIF-8. Compared with platinum/zeolite Y, it has super high dispersibility; it not only significantly increases the adsorption capacity of nitric oxide, but also effectively increases the conversion rate of nitric oxide at very low temperatures.

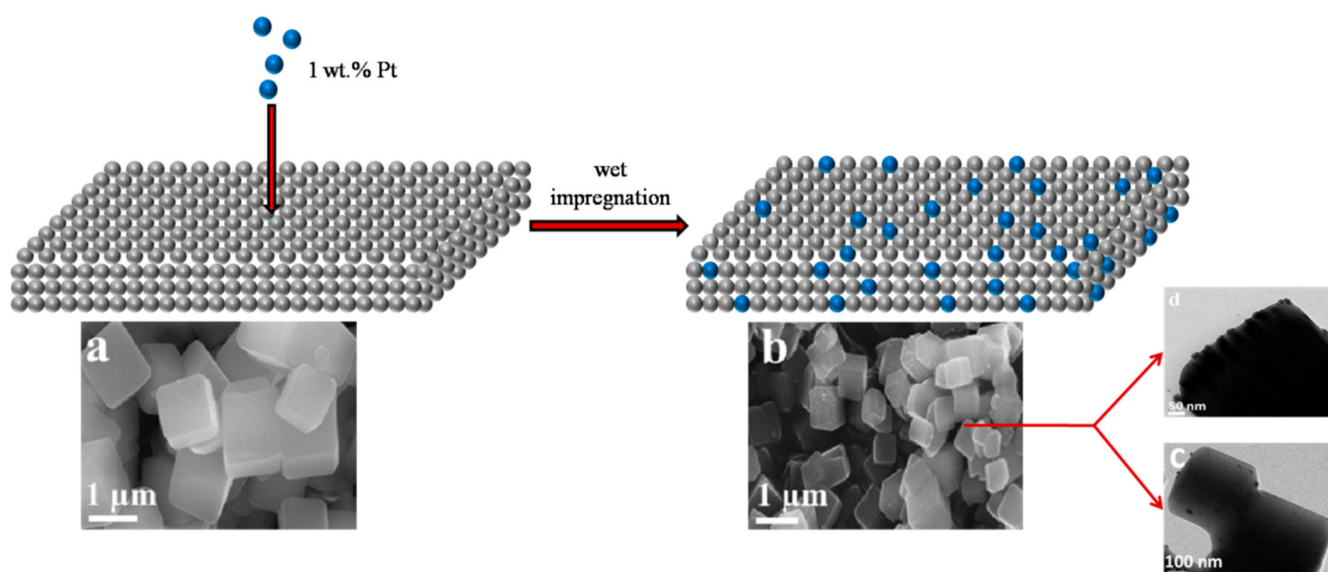


**Figure 6.** FE-SEM images of (a) ZIF-8 and (b) 1% Pt/ZIF-8, HR-TEM images of (c) 1% Pt/ZIF-8 with 50 nm scale and (d) 1% Pt/ZIF-8 with 100 nm scale [90].

Hydrogen was subjected to NO removal experiments on a Pt-W/HZSM-5 catalyst, and the NO<sub>x</sub> conversion rate reached a maximum at 110 °C. The characterization results showed that although both W and Pt tend to be dispersed on the support by occupying the Brønsted acid sites. However, when they coexist in the catalyst, the two synergistically occur preferentially. The synergistic effect of W and Pt not only facilitates the Pt to exhibit a metallic state in the catalyst, but also increases the dissociation speed of NO and H<sub>2</sub> on Pt while inhibiting the formation of nitrate [89]. Zhang et al. [91] prepared Pt/HY catalyst by impregnation method, and the loading amounts of Pt were 0.1, 0.2, 0.5, and 1.0 wt.%. The test results showed that the NO<sub>x</sub> conversion rate is the highest at 130 °C on a 0.5 wt.% Pt/HY catalyst with an oxygen concentration of 10%. Characterization revealed that the reaction of adsorbed H to reduce nitrite species happened at the junction of the Pt surface and the Pt carrier. In the Pt/H-FER catalyst, the temperature conditions required for NO<sub>x</sub> reduction and NO oxidation are reversed [96]. Xu et al. [92] synthesized aluminate spinel catalysts by sol-gel spontaneous ignition method. The test results showed that the Pd substituted aluminate spinel catalyst has excellent NO removal performance. Under the same reaction conditions, its activity is significantly better than the pure aluminate spinel catalyst. The incorporation of Pd into the aluminate spinel oxide significantly increases its catalytic activity and expands the active temperature window. Furthermore, the pure aluminate spinel catalyst and the palladium-doped aluminate spinel catalyst follow the same sequence of activity, indicating that the divalent metal is the key to design and improve the activity of the spinel catalyst.

Regarding the metal oxide catalyst, the nature and type of the oxide have a great influence on the reactivity of the catalyst. In Pt/MnO<sub>x</sub> and Pt/SiO<sub>2</sub> catalysts, MnO<sub>x</sub> and Pt/SiO<sub>2</sub> are inactive in low temperature NO removal by H<sub>2</sub> tests, but Pt/MnO<sub>x</sub> exhibits high catalytic activity [88]. Simultaneous loading of precious metals and non-noble metal elements on the catalyst may result in synergy between them. This method can reduce the experimental cost by adding a non-precious metal element to reduce the amount of precious metal added, while the catalytic activity remains substantially unchanged. Among the Ni<sub>10</sub>/Al<sub>2</sub>O<sub>3</sub>, Ni<sub>10</sub>/Pd<sub>0.5</sub>/Al<sub>2</sub>O<sub>3</sub>, and Ni<sub>10</sub>/Rh<sub>0.5</sub>/Al<sub>2</sub>O<sub>3</sub> catalysts, the most effective catalyst is Ni-Pd/Al<sub>2</sub>O<sub>3</sub>. Characterization results have revealed that the reduction of NiO in the catalyst precursor and the dispersion of the metal on the catalyst surface can be promoted with a small amount of Pd or Rh [97]. Zhou et al. [98] solved the problem of the narrow H<sub>2</sub>-SCR reaction temperature window by adding Pd to Mn/Ti and Au/Ti. PdAu catalyst

has good catalytic activity at 150–400 °C. PdMn also widens the reaction temperature window and has better catalytic activity than single metal catalyst.

The preparation of the catalyst by the inkjet printing process is a novel catalyst preparation method, and the design of the catalyst can be realized by printing. Chatziiona et al. [99] used the inkjet printing process to prepare Pt/Al<sub>2</sub>O<sub>3</sub> catalyst. The catalyst prepared by this method has excellent catalytic performance in a very low temperature range. This may be due to the formation of a unique catalyst surface structure during the printing process, which facilitates the formation of different NO<sub>x</sub> active intermediates. The characterization results showed that the printed Pt/Al<sub>2</sub>O<sub>3</sub> catalyst has a relatively uniform nano-spherical structure. Duan et al. [100] prepared new Pd-Au/TiO<sub>2</sub>, Pd/TiO<sub>2</sub>, and Au/TiO<sub>2</sub> catalysts by equal volume impregnation method. The test results showed that the Pd-Au/TiO<sub>2</sub> catalyst exhibits higher catalytic activity in a wide temperature window than the other two catalysts. The synergy between Pd and Au contributes to the formation of PdO and Pd–Au alloys, thereby promoting the progress of the NO<sub>x</sub> reduction reaction. Hu et al. [101] added nickel to Pd/TiO<sub>2</sub> catalyst and found that it had good catalytic activity in the presence of O<sub>2</sub>. The experimental results showed that the addition of nickel increases the reaction distance and reaction rate of hydrogen, and the addition of nickel in Pd/TiO<sub>2</sub> can generate more active single tooth ligand nitrate and enhance the activity of double tooth ligand nitrate. Zhang et al. [102] studied the performance of mixed metal oxides derived from binary layered double hydroxide as platinum-based catalyst carrier. They found that 0.1Pt/Mg<sub>3</sub>Al<sub>1</sub>O<sub>x</sub> catalyst appears with high catalytic activity at low temperature (200–220 °C), and the NO removal rate could reach more than 90%. It was also found that 0.1Pt/Mg<sub>3</sub>Al<sub>1</sub>O<sub>x</sub> manifest the highest catalytic activity, while 0.1 Pt/Ni<sub>3</sub>Al<sub>1</sub>O<sub>x</sub> has a high N<sub>2</sub> selectivity.

Perovskite-type composite oxide (ABO<sub>3</sub>) has good redox properties, good thermal stability, and low cost. It can be used for the reaction of NO removal, which is a promising catalyst. In a series of LaNi<sub>1-x</sub>Fe<sub>x</sub>O<sub>3</sub> (x = 0, 0.2, 0.4, 0.7, and 1.0) catalysts, the NO removal activity test found that the activity of the undoped LaNiO<sub>3</sub> catalyst is poor, while the activity of LaNi<sub>0.6</sub>Fe<sub>0.4</sub>O<sub>3</sub> catalyst is the highest. At each test temperature, LaFeO<sub>3</sub> has a higher NO<sub>x</sub> conversion than LaNiO<sub>3</sub>. Therefore, the Fe species promotes the catalytic performance of the catalyst. Characterization found that proper addition of iron can enhance the thermal stability and surface area of the catalyst [103]. Furfori et al. [93] prepared a series of perovskite catalysts (LaFeO<sub>3</sub>, La<sub>0.8</sub>Sr<sub>0.2</sub>FeO, Pd/La<sub>0.8</sub>Sr<sub>0.2</sub>FeO, La<sub>0.8</sub>Sr<sub>0.2</sub>Fe<sub>0.9</sub>Pd<sub>0.1</sub>O<sub>3</sub>, La<sub>0.7</sub>Sr<sub>0.2</sub>Ce<sub>0.1</sub>FeO<sub>3</sub>, Pd/La<sub>0.7</sub>Sr<sub>0.2</sub>Ce<sub>0.1</sub>FeO, La<sub>0.7</sub>Sr<sub>0.2</sub>-Ce<sub>0.1</sub>Fe<sub>0.9</sub>Pd<sub>0.1</sub>O<sub>3</sub>) by combustion synthesis process. It was found that the La<sub>0.8</sub>Sr<sub>0.2</sub>Fe<sub>0.9</sub>Pd<sub>0.1</sub>O<sub>3</sub> perovskite oxide was observed to have the highest catalytic activity.

#### 4.2. New Carrier

Due to excellent thermal stability and/or easy to dope other components, some new carriers have attracted much attention, which include MOFs [104], cobalt-doped nanoporous nickel phosphate VSB-5 [105], SBA-15 and MCM-41 [106,107], sulfasalazine (SSZ) [108], and carbon paper [109], etc. In addition, the traditional metal oxide carriers could be combined to form a new carrier, which has better catalytic performance compared to its parent carrier [110–114], if a right synthesis recipe is used.

MOFs are stable materials with organic and inorganic pores and has a high surface area. Aluminum-based MOFs exhibit excellent thermal stability due to the unique octahedron and strong Al-O bonds in the center of the aluminum. Xue et al. [104] prepared Pt<sub>x</sub>/MIL-96 catalysts with different Pt contents (x = 0.03, 0.11, 0.27, and 0.41) by hydrothermal method. Among them, the highest activity is Pt<sub>5</sub>/MIL-96/CP, and the NO removal rate can reach 100% at 60 °C. The characterization results showed that the high NO removal rate is attributed to the uniform deposition of Pt particles in MIL-96 and the synergy between Pt particles and MIL-96. At the same time, the high surface area and porosity of the MIL-96 carrier make it easier for H<sub>2</sub> and NO to reach the Pt site, which is essential for the removal of NO. Cobalt-doped nanoporous nickel phosphate VSB-5 is a recently developed catalyst [105]. The Co/VSB-5 catalyst has better activity than the undoped

Ni/VSB-5 catalyst. This is because the surface of Co/VSB-5 can adsorb a large amount of NO. The activity of the Co/VSB-5 catalyst is closely related to the cobalt loading, and the Co<sub>20</sub>/VSB-5 catalyst has the highest catalytic efficiency.

Both SBA-15 and MCM-41 are ordered mesoporous molecular sieves with uniform pore size, large specific surface area, and stable framework structure. They are easy to dope other components, and they also have better hydrothermal stability than other molecular sieves. In the experiments of two high-activity Pd-based catalysts (Pd/V<sub>2</sub>O<sub>5</sub>/TiO<sub>2</sub>/SBA-15 and Pd/V<sub>2</sub>O<sub>5</sub>/TiO<sub>2</sub>/MCM-41), the reduction of NO is catalyzed by H<sub>2</sub>, although the surface area of the SBA-15 supported catalyst is small. However, it showed a higher NO conversion rate in the catalyst performance test [106]. Yin et al. [107] prepared Pd/V<sub>2</sub>O<sub>5</sub>/TiO<sub>2</sub>/SBA-15 and Pd/V<sub>2</sub>O<sub>5</sub>/TiO<sub>2</sub>/MCM-41 catalysts, both of which showed good NO removal activity. Ryou et al. [108] chose sulfasalazine (SSZ) as the carrier to prepare Pd/SSZ-13 catalysts with different palladium contents by initial impregnation method, wet impregnation, ion exchange method, and solid ion exchange method. Among these four methods, ion exchange of Pd in SSZ-13 is very difficult to conduct. The Pd/SSZ-13 catalyst was subjected to hydrothermal aging treatment (HTA), and it was found that the NO adsorption capacity of the catalyst was enhanced. Through the NO adsorption-desorption results, the authors confirmed that HTA treatment is a key process for the catalyst to produce low temperature adsorption activity.

Cao et al. [109] prepared a new ultrafine Pt/Beta catalyst with carbon paper as the carrier. The experimental results showed that 0.8 wt.% Pt/Beta catalyst could achieve nearly 100% NO<sub>x</sub> conversion under the oxygen-rich condition at 90 °C. The dispersion and particle size of Pt were adjusted by using polyvinyl pyrrolidone (PVP) as dispersant. The results showed that when the amount of Pt is less than 50 mg, the particle size of Pt is smaller, the dispersion is larger, and the NO removal is higher. However, when the amount of Pt is more than 50 mg, the NO removal does not increase, and the activity decreases slightly.

The traditional carrier can be combined to form a new carrier, and better catalytic performance can be obtained. Among the W-CeO<sub>2</sub>-ZrO<sub>2</sub> catalysts with different carrier contents, one is 85 wt.% CeO<sub>2</sub>, 15 wt.% ZrO<sub>2</sub>, which is labeled as W-ZrCe; the other is 17 wt.% CeO<sub>2</sub>, 83 wt.% ZrO<sub>2</sub>, which is recorded as W-CeZr. The NO<sub>x</sub> conversion rate occurs most at the W-ZrCe catalyst at 300 °C. Under the same reaction conditions, the NO<sub>x</sub> conversion of the W-ZrCe catalyst is higher than that of W-CeZr [110]. A series of Pt/Ce<sub>x</sub>Zr<sub>1-x</sub>O<sub>2-δ</sub> (x = 0.4–0.6) catalysts were synthesized by Kalamaras [111], and the catalysts showed significant differences in NO conversion. Adding an auxiliary agent can effectively increase the activity of the catalyst. In the Pt/TiO<sub>2</sub> and Pt-WO<sub>3</sub>/TiO<sub>2</sub> catalysts, the addition of WO<sub>3</sub> significantly enhances the low temperature activity of the Pt/TiO<sub>2</sub> catalyst. This is due to the synergistic effect between Pt and WO<sub>3</sub>, which not only makes the adsorbed NO<sub>x</sub> species unstable, but also promotes the overflow of activated H [112]. Olympiou et al. [115] prepared the novel Pt nanocatalyst supported on MgO-CeO<sub>2</sub>. The new catalyzer has a superior performance on NO removal by H<sub>2</sub> with 90% conversion of NO and 80% N<sub>2</sub> selectivity in the low-temperature range of 120–180 °C for a wide range of O<sub>2</sub>, H<sub>2</sub>, and CO<sub>2</sub> feed concentrations. In the meantime, this catalytic system had been tested under industrial process conditions of NO<sub>x</sub> control and showed remarkable performance. Patel et al. [113] prepared a series of mixed metal oxide catalysts by coprecipitation followed by impregnation of palladium metal. The catalysts are denoted as Pd/MgO-CeO<sub>2</sub>, Pd/ZrO<sub>2</sub>-CeO<sub>2</sub>, Pd/Al<sub>2</sub>O<sub>3</sub>-CeO<sub>2</sub>, and Pd/TiO<sub>2</sub>-CeO<sub>2</sub>; the characterization results (Figure 7) show that only the addition of magnesium oxide and zirconium oxide improves the dispersibility of crystalline nanoparticles. Compared with the two noble metal catalysts, the NO<sub>x</sub> conversion rate of Zn/ZSM-5 catalyst reached the highest value at 250 °C in the catalysts Zn/ZSM-5, Pd-Zn/ZSM-5, and Pd-Ru-W/(ZrO<sub>2</sub>-SiO<sub>2</sub>)SO<sub>4</sub>. The TPD results indicated that the activity of Zn/ZSM is attributed to the presence of Zn<sup>2+</sup> ions in the backbone [114].

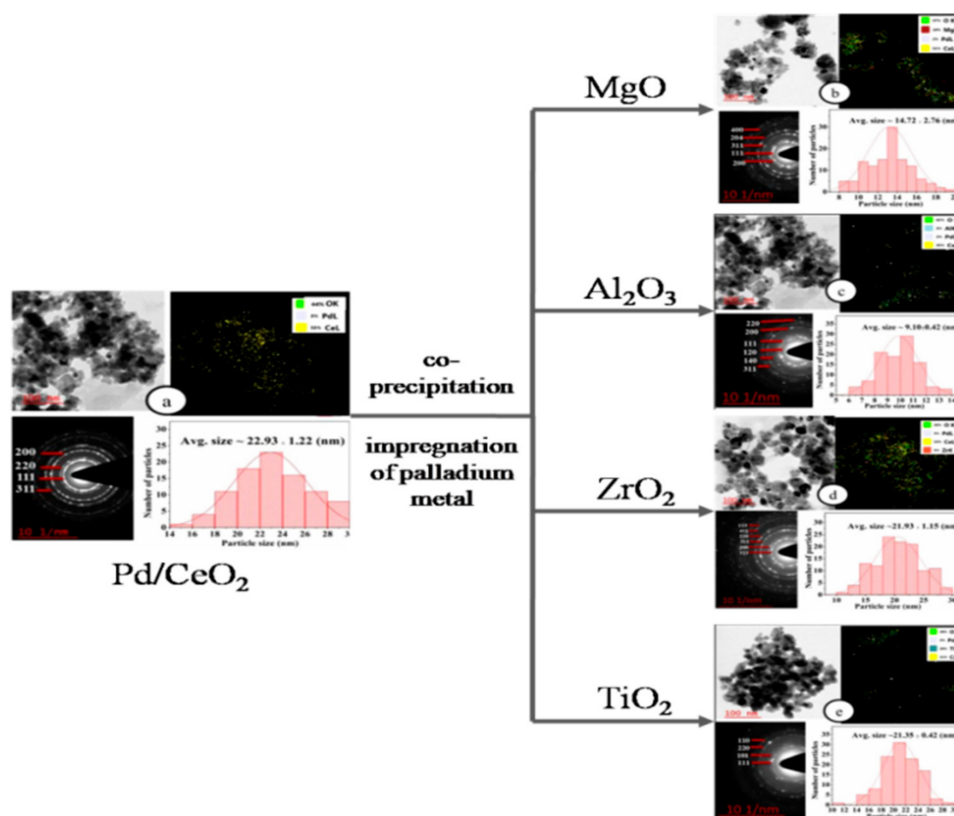


**Figure 7.** TEM micrograph of all the catalysts: (a) Pd/CeO<sub>2</sub>, (b) Pd/MgO-CeO<sub>2</sub>, (c) Pd/Al<sub>2</sub>O<sub>3</sub>-CeO<sub>2</sub>, (d) Pd/ZrO<sub>2</sub>-CeO<sub>2</sub>, (e) Pd/TiO<sub>2</sub>-CeO<sub>2</sub> [113].

#### 4.3. Reaction Mechanism

In the process of investigating, the mechanism of NO removal by H<sub>2</sub>, most of the researchers used infrared spectroscopy, ultraviolet spectroscopy, mass spectrometry, and steady-state isotope transient kinetic analysis to characterize the intermediates produced during the reaction. In this paper, two representative catalysts, Co/VSB-15 and Pd(111), are selected to discuss the reaction mechanism of NO removal by H<sub>2</sub> process as shown in Figure 8. It is generally believed that the principle of NO<sub>x</sub> reduction by H<sub>2</sub> is closely related to the nature of the catalyst itself. The reaction mechanism of different catalysts may be completely different. However, even for a particular catalyst, the mechanism of NO removal by H<sub>2</sub> is still affected by many factors such as reaction conditions and preparation methods.

Figure 8a describes a general process of NO removal by H<sub>2</sub> over Co-VSB-15 catalyst [105]. Gaseous NO is adsorbed on the surface of the catalyst, the active components NO<sub>(ad)</sub> and H<sub>(ad)</sub> can react with each other, and NO<sub>(ad)</sub>+H<sub>(ad)</sub>⇌N-OH<sub>(ad)</sub>⇌N<sub>(ad)</sub>+OH<sub>(ad)</sub> can occur continuously. The more active N<sub>(ad)</sub> components generated will react with each other and form N<sub>2</sub>. On the other hand, NO<sub>(ad)</sub> may react with NO to form N<sub>2</sub>O. In addition, some of the formed N<sub>2</sub>O may also adsorb on the catalyst surface. The adsorbed N<sub>2</sub>O<sub>(ad)</sub> can continuously react with the active H<sub>(ad)</sub> to form N<sub>2</sub> and H<sub>2</sub>O.

Figure 8b describes a simplified process of NO removal by H<sub>2</sub> over Pd(111) catalyst [18]. The dissociation of H<sub>2</sub> to atomic H is highly disfavored on clean Pd(111) surface due to high-energy barrier and endothermicity. Once H<sub>2</sub> is adsorbed on surface, the surface is covered with H atoms. When NO and H are co-adsorbed on the surface, there are five pathways possibly occurring for NO dissociation, as shown in Figure 8b. The presence of H atom facilitates the N–O bond scission via two abstraction reaction pathways, NO<sub>(ad)</sub>+H<sub>(ad)</sub>→NH<sub>(ad)</sub>+O<sub>(ad)</sub> and NO<sub>(ad)</sub>+H<sub>(ad)</sub>→N<sub>(ad)</sub>+OH<sub>(ad)</sub>, because of lower energy barriers of 1.68 and 1.58 eV, which are much lower than that of NO direct dissociation on its clean surface. The formation path of N<sub>2</sub> is NO<sub>(ad)</sub>+N<sub>(ad)</sub>→N<sub>2</sub>+O<sub>(ad)</sub> instead of

$N_{(ad)} + N_{(ad)} \rightarrow N_2$ . At the same time, the reaction product is mainly  $N_2O$  at low temperature. With the increase of temperature,  $N_2$  gradually becomes the main reaction product. In the meanwhile, an increased  $H_2$  pressure favors the formations of  $NH_3$  and  $H_2O$ . Thus, it is feasible to achieve high reduction reactivity of  $NO$  by  $H_2$  and selectivity of  $N_2$  over the Pd catalysts by controlling the reaction temperature and  $H_2$  pressure.

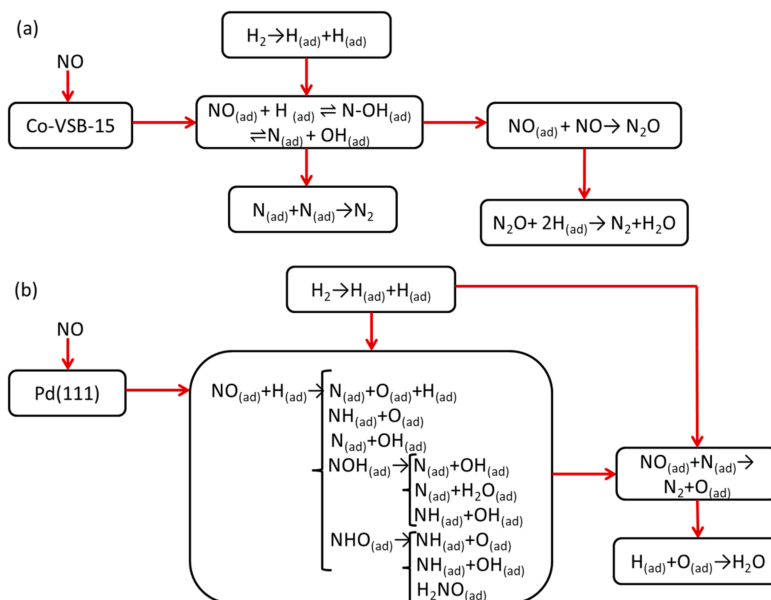


Figure 8. Possible mechanism of  $H_2+NO$  reaction over (a) Co/VSB-15 and (b) Pd(111) catalysts.

Table 3. Catalysts for catalytic reduction of  $NO_x$  by  $H_2$  under different conditions.

Catalyst	Maximum Conversion Temperature/ $^{\circ}C$	NO Conversion Rate/%	Reducing Agent	$O_2$ /%	$N_2$ Selectivity/%	Active Temperature Window/ $^{\circ}C$	GHSV/ $h^{-1}$	References
1%Pt/ZSM-35	120	80	5000 ppm $H_2$	6.7	72	75–150, 300–400	80,000	[94]
1%Pt/Beta	120	58	5000 ppm $H_2$	6.7	45	75–150, 300–400	80,000	[94]
0.5%Pt/H-FER	110	90	5000 ppm $H_2$	10	5	75–150	36,000	[96]
0.1 Pt/MgO–CeO <sub>2</sub>	140	99	0.8% $H_2$	2	94	120–180	33,000	[115]
0.1 Pt/MgO–CeO <sub>2</sub>	155	94	0.2% $H_2$	2	68	140–180	33,000	[115]
0.1 Pt/MgO–CeO <sub>2</sub>	155	97	0.4% $H_2$	2	82	120–180	33,000	[115]
Pt <sub>5</sub> MIL-96/CP	60	100	2% $H_2$	2		60–90		[104]
Pt <sub>1.5</sub> MIL-96/CP	90	75	2% $H_2$	2		70–90		[104]
Pt <sub>3</sub> MIL-96/CP	80	100	2% $H_2$	2		60–90		[104]
0.5%Pt–1%Cr/ZSM-35	120	95	0.5% $H_2$	6.7	66	100–180	80,000	[95]
0.5%Pt–2%Cr/ZSM-35	140	88	0.5% $H_2$	6.7	72	120–180	80,000	[95]

## 5. Summary and Outlook

To enhance quality of the living environment, the nitrogen oxides in the atmosphere need to be removed. At present, the SCR widely used in coal-fired power plants has obvious disadvantages. It is necessary to find other reducing agents to replace ammonia.  $CO$ ,  $CH_4$ , and  $H_2$  are the research hotspots in the field of catalysis, and also quite challenging research directions.

In the technology of  $NO$  removal by  $CO$  and  $CH_4$ , the catalysts are classified into two types: noble metal catalysts and non-precious metal catalysts. The former often has a high  $NO$  removal activity, but it has a disadvantage of poor hydrothermal stability at low temperatures. The latter is commonly cheaper, but the efficiency of  $NO$  removal is generally not high. The overall performance of non-precious metal catalysts can be improved by the addition of other metal elements or the use of novel supports. In the technology of  $NO$  removal by  $H_2$ , the  $NO$  removal performance of the noble metal catalyst is mainly

discussed from the traditional carrier and the new carrier. The present study discusses the activity enhancement methods of traditional supported catalysts such as molecular sieves, alumina, and zirconia, as well as the performance of new supported catalysts such as VSB-5, MOFs, and MCM-41. Recent research mainly focuses on the catalysts modification by loading different metal elements, doping active components, and changing preparation methods. Some progresses have been made in reducing the reaction temperature and improving the catalytic activity.

Regarding the catalytic reduction reaction of NO, it is generally believed that there are two models: one is the dissociative adsorption of NO, and the other is the reducing agent to reduce the adsorbed NO. In CO-SCR process, the key steps are the adsorption of NO<sub>x</sub> and the decomposition of NO. In CH<sub>4</sub>-SCR process, the activation of the C-H bond in CH<sub>4</sub> serves as a rate determining step of the reaction of NO removal. In the experiment of NO removal by CH<sub>4</sub>, NO<sub>x</sub> produced many nitrite, nitrate, and nitrosyl species on the noble metal active sites on the catalyst surface. In the H<sub>2</sub>-SCR process, the activation of the H-H bonds in H<sub>2</sub> serves as a rate determining step of the reaction of NO removal by H<sub>2</sub>. There are no solid conclusions about the types of three NO removal reactive intermediates. An in-depth study of the NO removal mechanism can lay a solid theoretical foundation for the improvement of the catalyst.

Many problems exist in the practical application of the technology of NO removal by CO and CH<sub>4</sub>. The technology of NO removal by CO has low activity under oxygen-rich conditions, and it is necessary to develop a new catalyst to adapt to the oxygen atmosphere. The activation of CH<sub>4</sub> is difficult, and NO removal conditions are harsh (reaction temperature >350 °C). The catalysts hardly adapt to those harsh working conditions, and further broadening of the reaction is required. Operating the temperature window to increase its low temperature activity to promote the activation of CH<sub>4</sub>, the reaction window of NO removal by H<sub>2</sub> is narrow; the combustion reaction of H<sub>2</sub> and O<sub>2</sub> at low temperature will reduce its ability to reduce NO. The existing catalysts are generally noble metal catalysts having high prices. In the industry, the treatment environment of nitrogen oxides is relatively harsh, and higher requirements are placed on the comprehensive performance of the catalyst.

Improvement of the catalyst for the above problems is the key to solving the industrial application of the catalyst. However, the improvement of the traditional catalyst has not made breakthrough progress. Referring to the catalyst preparation method of different reaction systems, the catalyst is required to be designed according to the mechanism of NO removal. The new carrier is used in the catalyst preparation process, which will have guiding significance for catalyst improvement. In the future, not only should the optimization of catalysts be strengthened to improve the performance of existing catalysts, but also new catalytic systems should be vigorously developed.

**Author Contributions:** J.S.: conceptualization, methodology, formal analysis, and writing—original draft preparation; Z.W.: conceptualization, methodology, formal analysis, and writing—review and editing; X.C.: conceptualization, methodology, writing—review and editing, and supervision; X.W.: conceptualization, methodology, and writing—review and editing. All authors have read and agreed to the published version of the manuscript.

**Funding:** This research was funded by the National Key R&D Program of China, grant number NO. 2017YFB0602904. The APC was funded by the National Key R&D Program of China (NO. 2017YFB0602904).

**Institutional Review Board Statement:** Not applicable.

**Informed Consent Statement:** Not applicable.

**Acknowledgments:** The authors thank the National Key R&D Program of China (NO. 2017YFB0602904) for the financial support.

**Conflicts of Interest:** The authors declare no conflict of interest.

## References

1. Liu, Z.; Ihl Woo, S. Recent advances in catalytic DeNOX science and technology. *Catal. Rev.* **2006**, *48*, 43–89. [[CrossRef](#)]
2. Han, L.; Cai, S.; Gao, M.; Hasegawa, J.-Y.; Wang, P.; Zhang, J.; Shi, L.; Zhang, D. Selective catalytic reduction of NO<sub>x</sub> with NH<sub>3</sub> by using novel catalysts: State of the art and future prospects. *Chem. Rev.* **2019**, *119*, 10916–10976. [[CrossRef](#)] [[PubMed](#)]
3. Gao, F.; Tang, X.; Yi, H.; Zhao, S.; Li, C.; Li, J.; Shi, Y.; Meng, X. A Review on Selective Catalytic Reduction of NO<sub>x</sub> by NH<sub>3</sub> over Mn-Based Catalysts at Low Temperatures: Catalysts, Mechanisms, Kinetics and DFT Calculations. *Catalyst* **2017**, *7*, 199. [[CrossRef](#)]
4. Deng, C.; Huang, Q.; Zhu, X.; Hu, Q.; Su, W.; Qian, J.; Dong, L.; Li, B.; Fan, M.; Liang, C. The influence of Mn-doped CeO<sub>2</sub> on the activity of CuO/CeO<sub>2</sub> in CO oxidation and NO + CO model reaction. *Appl. Surf. Sci.* **2016**, *389*, 1033–1049. [[CrossRef](#)]
5. Broqvist, P.; Panas, I.; Persson, H. A DFT study on CO oxidation over Co<sub>3</sub>O<sub>4</sub>. *J. Catal.* **2002**, *210*, 198–206. [[CrossRef](#)]
6. Hu, Y.; Dong, L.; Shen, M.; Liu, D.; Wang, J.; Ding, W.; Chen, Y. Influence of supports on the activities of copper oxide species in the low-temperature NO+CO reaction. *Appl. Catal. B Environ.* **2001**, *31*, 61–69. [[CrossRef](#)]
7. Mendes, A.N.; Matyenia, A.; Toullec, A.; Capela, S.; Ribeiro, M.F.; Henriques, C.; Da Costa, P. Potential synergic effect between MOR and BEA zeolites in NO<sub>x</sub> SCR with methane: A dual bed design approach. *Appl. Catal. A Gen.* **2015**, *506*, 246–253. [[CrossRef](#)]
8. Pan, H.; Jian, Y.; Yu, Y.; Chen, N.; He, C.; He, C. Promotional mechanism of propane on selective catalytic reduction of NO<sub>x</sub> by methane over In/H-BEA at low temperature. *Appl. Surf. Sci.* **2016**, *390*, 608–616. [[CrossRef](#)]
9. Hu, Z.; Yang, R.T. 110th Anniversary: Recent Progress and Future Challenges in Selective Catalytic Reduction of NO by H<sub>2</sub> in the Presence of O<sub>2</sub>. *Ind. Eng. Chem. Res.* **2019**, *58*, 10140–10153. [[CrossRef](#)]
10. Hong, Z.; Wang, Z.; Chen, D.; Sun, Q.; Li, X. Hollow ZSM-5 encapsulated Pt nanoparticles for selective catalytic reduction of NO by hydrogen. *Appl. Surf. Sci.* **2018**, *440*, 1037–1046. [[CrossRef](#)]
11. Cheng, X.; Zhang, X.; Su, D.; Wang, Z.; Chang, J.; Ma, C. NO reduction by CO over copper catalyst supported on mixed CeO<sub>2</sub> and Fe<sub>2</sub>O<sub>3</sub>: Catalyst design and activity test. *Appl. Catal. B Environ.* **2018**, *239*, 485–501. [[CrossRef](#)]
12. Higo, T.; Omori, Y.; Shigemoto, A.; Ueno, K.; Ogo, S.; Sekine, Y. Promotive effect of H<sub>2</sub>O on low-temperature NO reduction by CO over Pd/La<sub>0.9</sub>Ba<sub>0.1</sub>AlO<sub>3-δ</sub>. *Catal. Today* **2020**, *352*, 192–197. [[CrossRef](#)]
13. Lin, R.; Su, Y.; Cheng, J.; Zhang, X.; Wen, N.; Deng, W.; Zhou, H.; Zhao, B. Performance of Fe/Ga<sub>2</sub>O<sub>3</sub>-Al<sub>2</sub>O<sub>3</sub> catalysts on methane selective catalysis and NO reduction. *Chin. J. Environ. Eng.* **2020**, *14*, 1592–1604.
14. Li, Z. *Study on Poisoning and Anti-Positioning Mechanism of CH<sub>4</sub>-SCR on In/H-Beta Catalyst*; Harbin Institute of Technology: Harbin, China, 2019.
15. Sierra-Pereira, C.A.; Urquieta-González, E.A. Reduction of NO with CO on CuO or Fe<sub>2</sub>O<sub>3</sub> catalysts supported on TiO<sub>2</sub> in the presence of O<sub>2</sub>, SO<sub>2</sub> and water steam. *Fuel* **2014**, *118*, 137–147. [[CrossRef](#)]
16. Yang, H.-Q.; Fu, H.-Q.; Su, B.-F.; Xiang, B.; Xu, Q.-Q.; Hu, C.-W. Theoretical Study on the Catalytic Reduction Mechanism of NO by CO on Tetrahedral Rh<sub>4</sub> Subnanocluster. *J. Phys. Chem. A* **2015**, *119*, 11548–11564. [[CrossRef](#)] [[PubMed](#)]
17. Lónyi, F.; Solt, H.E.; Pászti, Z.; Valyon, J. Mechanism of NO-SCR by methane over Co,H-ZSM-5 and Co,H-mordenite catalysts. *Appl. Catal. B Environ.* **2014**, *150–151*, 218–229. [[CrossRef](#)]
18. Huai, L.-Y.; He, C.-Z.; Wang, H.; Wen, H.; Yi, W.-C.; Liu, J.-Y. NO dissociation and reduction by H<sub>2</sub> on Pd (111): A first-principles study. *J. Catal.* **2015**, *322*, 73–83. [[CrossRef](#)]
19. Li, J.; Wang, S.; Zhou, L.; Luo, G.; Wei, F. NO reduction by CO over a Fe-based catalyst in FCC regenerator conditions. *Chem. Eng. J.* **2014**, *255*, 126–133. [[CrossRef](#)]
20. Kudo, S.; Maki, T.; Yamada, M.; Mae, K. A new preparation method of Au/ferric oxide catalyst for low temperature CO oxidation. *Chem. Eng. Sci.* **2010**, *65*, 214–219. [[CrossRef](#)]
21. Hosokawa, S.; Matsuki, K.; Tamaru, K.; Oshino, Y.; Aritani, H.; Asakura, H.; Teramura, K.; Tanaka, T. Selective reduction of NO over Cu/Al<sub>2</sub>O<sub>3</sub>: Enhanced catalytic activity by infinitesimal loading of Rh on Cu/Al<sub>2</sub>O<sub>3</sub>. *Mol. Catal.* **2017**, *442*, 74–82. [[CrossRef](#)]
22. Liotta, L.; Pantaleo, G.; Di Carlo, G.; Marci, G.; Deganello, G. Structural and morphological investigation of a cobalt catalyst supported on alumina-baria: Effects of redox treatments on the activity in the NO reduction by CO. *Appl. Catal. B Environ.* **2004**, *52*, 1–10. [[CrossRef](#)]
23. Salker, A.; Desai, M.F. Catalytic activity and mechanistic approach of NO reduction by CO over M<sub>0.05</sub>Co<sub>2.95</sub>O<sub>4</sub> (M = Rh, Pd & Ru) spinel system. *Appl. Surf. Sci.* **2016**, *389*, 344–353. [[CrossRef](#)]
24. Ding, W.; Li, W. First-principles study of NO reduction by CO on transition metal atoms-doped CeO<sub>2</sub>(111). *Chin. J. Catal.* **2014**, *35*, 1937–1943. [[CrossRef](#)]
25. Sui, C.; Yuan, F.; Zhang, Z.; Wang, N.; Niu, X.; Zhu, Y. Catalytic activity of Ru/La<sub>1.6</sub>Ba<sub>0.4</sub>NiO<sub>4</sub> perovskite-like catalyst for NO + CO reaction: Interaction between Ru and La<sub>1.6</sub>Ba<sub>0.4</sub>NiO<sub>4</sub>. *Mol. Catal.* **2017**, *437*, 37–46. [[CrossRef](#)]
26. Oton, L.F.; Oliveira, A.C.; de Araujo, J.C.S.; Araujo, R.S.; de Sousa, F.F.; Saraiva, G.D.; Lang, R.; Otubo, L.; Carlos da Silva Duarte, G.; Campos, A. Selective catalytic reduction of NO<sub>x</sub> by CO (CO-SCR) over metal-supported nanoparticles dispersed on porous alumina. *Adv. Powder Technol.* **2020**, *31*, 464–476. [[CrossRef](#)]
27. Wu, S.; Li, X.; Fang, X.; Sun, Y.; Sun, J.; Zhou, M.; Zang, S. NO reduction by CO over TiO<sub>2</sub>-γ-Al<sub>2</sub>O<sub>3</sub> supported In/Ag catalyst under lean burn conditions. *Chin. J. Catal.* **2016**, *37*, 2018–2024. [[CrossRef](#)]
28. Ilieva, L.; Pantaleo, G.; Velinov, N.; Tabakova, T.; Petrova, P.; Ivanov, I.; Avdeev, G.; Paneva, D.; Venezia, A.M. NO reduction by CO over gold catalysts supported on Fe-loaded ceria. *Appl. Catal. B Environ.* **2015**, *174–175*, 176–184. [[CrossRef](#)]

29. Huang, K.; Lin, L.; Yang, K.; Dai, W.; Chen, X.; Fu, X. Promotion effect of ultraviolet light on NO + CO reaction over Pt/TiO<sub>2</sub> and Pt/CeO<sub>2</sub>-TiO<sub>2</sub> catalysts. *Appl. Catal. B Environ.* **2015**, *179*, 395–406. [[CrossRef](#)]
30. Ferrer, V.; Finol, D.; Solano, R.; Moronta, A.; Ramos, M. Reduction of NO by CO using Pd-CeTb and Pd-CeZr catalysts supported on SiO<sub>2</sub> and La<sub>2</sub>O<sub>3</sub>-Al<sub>2</sub>O<sub>3</sub>. *J. Environ. Sci.* **2015**, *27*, 87–96. [[CrossRef](#)]
31. Wang, X.; Wu, X.; Maeda, N.; Baiker, A. Striking activity enhancement of gold supported on Al-Ti mixed oxide by promotion with ceria in the reduction of NO with CO. *Appl. Catal. B Environ.* **2017**, *209*, 62–68. [[CrossRef](#)]
32. Shin, H.U.; Lolla, D.; Nikolov, Z.; Chase, G.G. Pd-Au nanoparticles supported by TiO<sub>2</sub> fibers for catalytic NO decomposition by CO. *J. Ind. Eng. Chem.* **2016**, *33*, 91–98. [[CrossRef](#)]
33. Liotta, L.; Deganello, G.; Sannino, D.; Gaudino, M.; Ciambelli, P.; Gialanella, S. Influence of barium and cerium oxides on alumina supported Pd catalysts for hydrocarbon combustion. *Appl. Catal. A Gen.* **2002**, *229*, 217–227. [[CrossRef](#)]
34. Sun, J.; Ge, C.; Yao, X.; Zou, W.; Hong, X.; Tang, C.; Dong, L. Influence of different impregnation modes on the properties of CuO/CeO<sub>2</sub>/γ-Al<sub>2</sub>O<sub>3</sub> catalysts for NO reduction by CO. *Appl. Surf. Sci.* **2017**, *426*, 279–286. [[CrossRef](#)]
35. Zhang, L.; Yao, X.; Lu, Y.; Sun, C.; Tang, C.; Gao, F.; Dong, L. Effect of precursors on the structure and activity of CuO-CoOx/γ-Al<sub>2</sub>O<sub>3</sub> catalysts for NO reduction by CO. *J. Colloid Interface Sci.* **2018**, *509*, 334–345. [[CrossRef](#)] [[PubMed](#)]
36. Cha, B.J.; Kim, I.H.; Park, C.H.; Choi, C.M.; Sung, J.Y.; Choi, M.C.; Kim, Y.D. Reduction of NO by CO catalyzed by Fe-oxide/Al<sub>2</sub>O<sub>3</sub>: Strong catalyst-support interaction for enhanced catalytic activity. *Appl. Surf. Sci.* **2020**, *509*. [[CrossRef](#)]
37. Boningari, T.; Pavani, S.M.; Ettireddy, P.R.; Chuang, S.S.; Smirniotis, P.G. Mechanistic investigations on NO reduction with CO over Mn/TiO<sub>2</sub> catalyst at low temperatures. *Mol. Catal.* **2018**, *451*, 33–42. [[CrossRef](#)]
38. Zhang, X.; Ma, C.; Cheng, X.; Wang, Z. Performance of Fe-Ba/ZSM-5 catalysts in NO + O<sub>2</sub> adsorption and NO + CO reduction. *Int. J. Hydrogen Energy* **2017**, *42*, 7077–7088. [[CrossRef](#)]
39. Yoshida, H.; Okabe, Y.; Yamashita, N.; Hinokuma, S.; Machida, M. Catalytic CO-NO reaction over Cr-Cu embedded CeO<sub>2</sub> surface structure. *Catal. Today* **2017**, *281*, 590–595. [[CrossRef](#)]
40. Savereide, L.; Gosavi, A.; Hicks, K.E.; Notestein, J.M. Identifying properties of low-loaded CoOx/CeO<sub>2</sub> via X-ray absorption spectroscopy for NO reduction by CO. *J. Catal.* **2020**, *381*, 355–362. [[CrossRef](#)]
41. Wang, X.; Lu, Y.; Tan, W.; Liu, A.; Ji, J.; Wan, H.; Sun, C.; Tang, C.; Dong, L. Insights into the precursor effect on the surface structure of γ-Al<sub>2</sub>O<sub>3</sub> and NO + CO catalytic performance of CO-pretreated CuO/MnOx/γ-Al<sub>2</sub>O<sub>3</sub> catalysts. *J. Colloid Interface Sci.* **2019**, *554*, 611–618. [[CrossRef](#)]
42. Xianrui, G.; Hao, L.; Lichen, L.; Changjin, T.; Fei, G.; Lin, D. Promotional effect of CO pretreatment on CuO/CeO<sub>2</sub> catalyst for catalytic reduction of NO by CO. *J. Rare Earths* **2014**, *32*, 139–145.
43. Zhang, S.; Lee, J.; Kim, D.H.; Kim, T. NO reduction by CO over CoOx/CeO<sub>2</sub> catalysts: Effect of support calcination temperature on activity. *Mol. Catal.* **2020**, *482*, 110703. [[CrossRef](#)]
44. Wang, L.; Cheng, X.; Wang, Z.; Ma, C.; Qin, Y. Investigation on Fe-Co binary metal oxides supported on activated semi-coke for NO reduction by CO. *Appl. Catal. B Environ.* **2017**, *201*, 636–651. [[CrossRef](#)]
45. Cheng, X.; Cheng, Y.; Wang, Z.; Ma, C. Comparative study of coal based catalysts for NO adsorption and NO reduction by CO. *Fuel* **2018**, *214*, 230–241. [[CrossRef](#)]
46. Du, Q.; Cheng, X.; Tahir, M.H.; Su, D.; Wang, Z.; Chen, S. Investigation on NO reduction by CO and H<sub>2</sub> over metal oxide catalysts Cu<sub>2</sub>M<sub>9</sub>CeO<sub>x</sub>. *Int. J. Hydrogen Energy* **2020**, *45*, 16469–16481. [[CrossRef](#)]
47. Wang, X.; Li, X.; Mu, J.; Fan, S.; Wang, L.; Gan, G.; Qin, M.; Li, J.; Li, Z.; Zhang, D. Facile Design of Highly Effective Cu<sub>x</sub>Co<sub>1-x</sub>O<sub>y</sub> Catalysts with Diverse Surface/Interface Structures toward NO Reduction by CO at Low Temperatures. *Ind. Eng. Chem. Res.* **2019**, *58*, 15459–15469. [[CrossRef](#)]
48. Yun, L.; Li, Y.; Zhou, C.; Lan, L.; Zeng, M.; Mao, M.; Liu, H.; Zhao, X. The formation of CuO/OMS-2 nanocomposite leads to a significant improvement in catalytic performance for NO reduction by CO. *Appl. Catal. A Gen.* **2017**, *530*, 1–11. [[CrossRef](#)]
49. Qin, Y.-H.; Huang, L.; Zheng, J.-X.; Ren, Q. Low-temperature selective catalytic reduction of NO with CO over A-Cu-BTC and AOx/CuOy/C catalyst. *Inorg. Chem. Commun.* **2016**, *72*, 78–82. [[CrossRef](#)]
50. Wang, Y.; Zhang, L.; Li, R.; He, H.; Wang, H.; Huang, L. MOFs-based coating derived Me-ZIF-67@ CuOx materials as low-temperature NO-CO catalysts. *Chem. Eng. J.* **2020**, *381*, 122757. [[CrossRef](#)]
51. Kacimi, M.; Ziyad, M.; Liotta, L.F. Cu on amorphous AlPO<sub>4</sub>: Preparation, characterization and catalytic activity in NO reduction by CO in presence of oxygen. *Catal. Today* **2015**, *241*, 151–158. [[CrossRef](#)]
52. Dharmarathna, S.; King'ondeu, C.K.; Pedrick, W.; Pahalagedara, L.; Suib, S.L. Direct Sonochemical Synthesis of Manganese Octahedral Molecular Sieve (OMS-2) Nanomaterials Using Cosolvent Systems, Their Characterization, and Catalytic Applications. *Chem. Mater.* **2012**, *24*, 705–712. [[CrossRef](#)]
53. Salker, A.; Desai, M.F. CO-NO/O<sub>2</sub> redox reactions over Cu substituted cobalt oxide spinels. *Catal. Commun.* **2016**, *87*, 116–119. [[CrossRef](#)]
54. Zhu, C.; Gong, Z.-J.; Jin, K.; Luo, H.-J.; Wu, W.-F. Research on Catalytic Denitrification Performance of Rare Earth Tailings in CO Atmosphere. *Rare Met. Cem. Carbides* **2019**, *47*, 25–32.
55. Wang, Y.; Zhu, A.; Zhang, Y.; Au, C.; Yang, X.; Shi, C. Catalytic reduction of NO by CO over NiO/CeO<sub>2</sub> catalyst in stoichiometric NO/CO and NO/CO/O<sub>2</sub> reaction. *Appl. Catal. B Environ.* **2008**, *81*, 141–149. [[CrossRef](#)]

56. Yao, X.; Xiong, Y.; Zou, W.; Zhang, L.; Wu, S.; Dong, X.; Gao, F.; Deng, Y.; Tang, C.; Chen, Z.; et al. Correlation between the physicochemical properties and catalytic performances of  $Ce_xSn_{1-x}O_2$  mixed oxides for NO reduction by CO. *Appl. Catal. B Environ.* **2014**, *144*, 152–165. [[CrossRef](#)]
57. Zou, W.; Liu, L.; Zhang, L.; Li, L.; Cao, Y.; Wang, X.; Tang, C.; Gao, F.; Dong, L. Crystal-plane effects on surface and catalytic properties of  $Cu_2O$  nanocrystals for NO reduction by CO. *Appl. Catal. A Gen.* **2015**, *505*, 334–343. [[CrossRef](#)]
58. Deng, C.; Li, B.; Dong, L.; Zhang, F.; Fan, M.; Jin, G.; Gao, J.; Gao, L.; Zhang, F.; Zhou, X. NO reduction by CO over CuO supported on  $CeO_2$ -doped  $TiO_2$ : The effect of the amount of a few  $CeO_2$ . *Phys. Chem. Chem. Phys.* **2015**, *17*, 16092–16109. [[CrossRef](#)]
59. Sakmeche, M.; Belhakem, A.; Kessas, R.; Ghomari, S.A. Effect of parameters on NO reduction by methane in presence of excess  $O_2$  and functionalized AlMCM-41 as catalysts. *J. Taiwan Inst. Chem. Eng.* **2017**, *80*, 333–341. [[CrossRef](#)]
60. Cano, M.; Guarín, F.; Aristizábal, B.; Villa, A.-L.; González, L.-M. Catalytic activity and stability of Pd/Co catalysts in simultaneous selective catalytic reduction of NOx with methane and oxidation of o-dichlorobenzene. *Catal. Today* **2017**, *296*, 105–117. [[CrossRef](#)]
61. Zhang, H.; Li, L.; Li, N.; Wang, A.; Wang, X.; Zhang, T. In situ FT-IR investigation on the selective catalytic reduction of NO with  $CH_4$  over Pd/sulfated alumina catalyst. *Appl. Catal. B Environ.* **2011**, *110*, 171–177. [[CrossRef](#)]
62. Azambre, B.; Zenboury, L.; Da Costa, P.; Capela, S.; Carpentier, S.; Westermann, A. Palladium catalysts supported on sulfated ceria-zirconia for the selective catalytic reduction of NOx by methane: Catalytic performances and nature of active Pd species. *Catal. Today* **2011**, *176*, 242–249. [[CrossRef](#)]
63. Decolatti, H.; Solt, H.; Lónyi, F.; Valyon, J.; Miró, E.; Gutiérrez, L. The role of Pd-In interactions on the performance of PdIn-Hmordenite in the SCR of NOx with  $CH_4$ . *Catal. Today* **2011**, *172*, 124–131. [[CrossRef](#)]
64. Sowade, T.; Liese, T.; Schmidt, C.; Schütze, F.-W.; Yu, X.; Berndt, H.; Grünert, W. Relations between structure and catalytic activity of Ce-In-ZSM-5 catalysts for the selective reduction of NO by methane: II. Interplay between the  $CeO_2$  promoter and different indium sites. *J. Catal.* **2004**, *225*, 105–115. [[CrossRef](#)]
65. Nakagawa, K.; Arai, Y.; Umezaki, Y.; Yoshida, A.; Kajiwara, Y.; Aoyagi, S.; Matsuyama, H.; Sugiyama, S. Template effect of phosphate surfactant on formation of hydroxyapatite nanostructures with various shapes. *Mater. Chem. Phys.* **2018**, *213*, 183–190. [[CrossRef](#)]
66. Zhao, J.; Zhang, G.; He, J.; Wen, Z.; Li, Z.; Gu, T.; Ding, R.; Zhu, Y.; Zhu, R. Effect of preparation and reaction conditions on the performance of In/H-Beta for selective catalytic reduction of NOx with  $CH_4$ . *Chemosphere* **2020**, *252*, 126458. [[CrossRef](#)]
67. Azizi, Y.; Kambolis, A.; Boréave, A.; Giroir-Fendler, A.; Retailleau-Mevel, L.; Guiot, B.; Marchand, O.; Walter, M.; Desse, M.-L.; Marchin, L.; et al. NOx abatement in the exhaust of lean-burn natural gas engines over Ag-supported  $\gamma-Al_2O_3$  catalysts. *Surf. Sci.* **2016**, *646*, 186–193. [[CrossRef](#)]
68. Mendes, A.N.; Zhobolbenko, V.L.; Thibault-Starzyk, F.; Da Costa, P.; Henriques, C. On the enhancing effect of Ce in Pd-MOR catalysts for NOx  $CH_4$ -SCR: A structure-reactivity study. *Appl. Catal. B Environ.* **2016**, *195*, 121–131. [[CrossRef](#)]
69. Sun, J.; Wang, Y.; Ma, Q.; Bin, L.; Zhao, Y.; Tian, Y.; Hong, W.; Chi, Y.; Cuiqing, L.; Yongji, S. Catalytic performance of Ag(x)/ZSM-5 catalysts for selective catalytic reduction of nitric oxide by methane. *J. Fuel Chem. Technol.* **2020**, *48*, 197–204.
70. Rodrigues, A.; da Costa, P.; Méthivier, C.; Dzwigaj, S. Controlled preparation of CoPdSiBEA zeolite catalysts for selective catalytic reduction of NO with methane and their characterisation by XRD, DR UV-vis, TPR, XPS. *Catal. Today* **2011**, *176*, 72–76. [[CrossRef](#)]
71. Costilla, I.O.; Sánchez, M.D.; Volpe, M.A.; Gigola, C.E. Ce effect on the selective catalytic reduction of NO with  $CH_4$  on Pd-mordenite in the presence of  $O_2$  and  $H_2O$ . *Catal. Today* **2011**, *172*, 84–89. [[CrossRef](#)]
72. Gómez-García, M.; Zimmermann, Y.; Pitchon, V.; Kiennemann, A. Multifunctional catalyst for de-NOx processes: The selective reduction of NOx by methane. *Catal. Commun.* **2007**, *8*, 400–404. [[CrossRef](#)]
73. Liu, Z.; Wang, K.; Zhang, X.; Wang, J.; Cao, H.; Gong, M.; Chen, Y. Study on methane selective catalytic reduction of NO on Pt/ $Ce_{0.67}Zr_{0.33}O_2$  and its application. *J. Nat. Gas Chem.* **2009**, *18*, 66–70. [[CrossRef](#)]
74. Li, H.; Jiang, X.; Zheng, X. Plasma-assisted CuO/ $CeO_2$ / $TiO_2$ - $\gamma-Al_2O_3$  catalysts for NO+ $CH_4$  reaction and NO temperature programmed desorption studies. *Appl. Surf. Sci.* **2013**, *280*, 273–281. [[CrossRef](#)]
75. Ren, L.L.; Zhang, T. Reduction of NO with methane over Fe/ZSM-5 catalysts. *Chin. Chem. Lett.* **2010**, *21*, 674–677. [[CrossRef](#)]
76. Su, Y.; Zhao, B.; Deng, W. NO reduction by methane over iron oxides: Characteristics and mechanisms. *Fuel* **2015**, *160*, 80–86. [[CrossRef](#)]
77. Campa, M.C.; Pietrogiamici, D.; Occhiuzzi, M. The simultaneous selective catalytic reduction of  $N_2O$  and NOx with  $CH_4$  on Co- and Ni-exchanged mordenite. *Appl. Catal. B Environ.* **2015**, *168*, 293–302. [[CrossRef](#)]
78. Hong, W.; Bin, L.; Lu, X.-B.; Li, C.-Q.; Ding, F.-C.; Song, Y.-J. Selective catalytic reduction of NO by methane over the Co/MOR catalysts in the presence of oxygen. *J. Fuel Chem. Technol.* **2015**, *43*, 1106–1112.
79. Janas, J.; Dzwigaj, S. Physico-chemical properties of FeAlBEA and FeSiBEA zeolites and their catalytic activity in the SCR of NO with ethanol or methane. *Catal. Today* **2011**, *176*, 272–276. [[CrossRef](#)]
80. Charrad, R.; Solt, H.E.; Domján, A.; Ayari, F.; Mhamdi, M.; Valyon, J.; Lónyi, F. Selective catalytic reduction of NO by methane over Co,H-SSZ-13 catalysts: Types and catalytic functions of active Co sites. *J. Catal.* **2020**, *385*, 87–102. [[CrossRef](#)]
81. Bin Lim, J.; Shin, J.; Ahn, N.H.; Heo, I.; Hong, S.B. Selective catalytic reduction of NO with  $CH_4$  over cobalt-exchanged cage-based, small-pore zeolites with different framework structures. *Appl. Catal. B Environ.* **2020**, *267*, 118710. [[CrossRef](#)]
82. Li, Y.; Su, J.; Ma, J.; Yu, F.; Chen, J.; Li, R. Novel straight synthesis of super-microporous Cu/ $Al_2O_3$  catalyst with high  $CH_4$ -SCR-NO activity. *Catal. Commun.* **2015**, *65*, 6–9. [[CrossRef](#)]

83. Li, N.; Wang, A.; Liu, Z.; Wang, X.; Zheng, M.; Huang, Y.; Zhang, T. On the catalytic nature of Mn/sulfated zirconia for selective reduction of NO with methane. *Appl. Catal. B Environ.* **2006**, *62*, 292–298. [[CrossRef](#)]
84. Chou, Z. *Experimental Study on the Denox Technology of CH<sub>4</sub>-SCR and Co-SCR Based on Copper-Based Catalyst*; North China Electric Power University: Beijing, China, 2018.
85. Sun, Z.; Xu, J.; Su, S.; Qing, M.; Wang, L.; Cui, X.; Mostafa, M.E.; Zhang, C.; Hu, S.; Wang, Y.; et al. Formation and re-duction of NO from the oxidation of NH<sub>3</sub>/CH<sub>4</sub> with high concentration of H<sub>2</sub>O. *Fuel* **2019**, *247*, 19–25. [[CrossRef](#)]
86. Jing, G.; Li, J.; Yang, D.; Hao, J. Promotional mechanism of tungsten on selective catalytic reduction of NO<sub>x</sub> by methane over In/WO<sub>3</sub>/ZrO<sub>2</sub>. *Appl. Catal. B Environ.* **2009**, *91*, 123–134. [[CrossRef](#)]
87. Li, X.; Zhang, X.; Xu, Y.; Liu, Y.; Wang, X. Influence of support properties on H<sub>2</sub> selective catalytic reduction activities and N<sub>2</sub> selectivities of Pt catalysts. *Chin. J. Catal.* **2015**, *36*, 197–203. [[CrossRef](#)]
88. Park, S.M.; Kim, M.-Y.; Kim, E.S.; Han, H.-S.; Seo, G. H<sub>2</sub>-SCR of NO on Pt–MnO<sub>x</sub> catalysts: Reaction path via NH<sub>3</sub> formation. *Appl. Catal. A Gen.* **2011**, *395*, 120–128. [[CrossRef](#)]
89. Zhang, X.; Wang, X.; Zhao, X.; Xu, Y.; Liu, Y.; Yu, Q. Promotion effect of tungsten on the activity of Pt/HZSM-5 for H<sub>2</sub>-SCR. *Chem. Eng. J.* **2015**, *260*, 419–426. [[CrossRef](#)]
90. Challagulla, S.; Payra, S.; Rameshan, R.; Roy, S. Low temperature catalytic reduction of NO over porous Pt/ZIF-8. *J. Environ. Chem. Eng.* **2020**, *8*, 103815. [[CrossRef](#)]
91. Zhang, X.; Wang, X.; Zhao, X.; Xu, Y.; Gao, H.; Zhang, F. An investigation on N<sub>2</sub>O formation route over Pt/HY in H<sub>2</sub>-SCR. *Chem. Eng. J.* **2014**, *252*, 288–297. [[CrossRef](#)]
92. Xu, C.; Sun, W.; Cao, L.; Li, T.; Cai, X.; Yang, J. Highly efficient Pd-doped aluminate spinel catalysts with different di-valent cations for the selective catalytic reduction of NO with H<sub>2</sub> at low temperature. *Chem. Eng. J.* **2017**, *308*, 980–987. [[CrossRef](#)]
93. Furfori, S.; Russo, N.; Fino, D.; Saracco, G.; Specchia, V. NO SCR reduction by hydrogen generated in line on perovskite-type catalysts for automotive diesel exhaust gas treatment. *Chem. Eng. Sci.* **2010**, *65*, 120–127. [[CrossRef](#)]
94. Yu, Q.; Richter, M.; Kong, F.; Li, L.; Wu, G.; Guan, N. Selective catalytic reduction of NO by hydrogen over Pt/ZSM-35. *Catal. Today* **2010**, *158*, 452–458. [[CrossRef](#)]
95. Yu, Q.; Richter, M.; Li, L.; Kong, F.; Wu, G.; Guan, N. The promotional effect of Cr on catalytic activity of Pt/ZSM-35 for H<sub>2</sub>-SCR in excess oxygen. *Catal. Commun.* **2010**, *11*, 955–959. [[CrossRef](#)]
96. Yang, S.; Wang, X.; Chu, W.; Song, Z.; Zhao, S. An investigation of the surface intermediates of H<sub>2</sub>-SCR of NO<sub>x</sub> over Pt/H-FER. *Appl. Catal. B Environ.* **2011**, *107*, 380–385. [[CrossRef](#)]
97. Mihet, M.; Lazar, M. Effect of Pd and Rh promotion on Ni/Al<sub>2</sub>O<sub>3</sub> for NO reduction by hydrogen for stationary applications. *Chem. Eng. J.* **2014**, *251*, 310–318. [[CrossRef](#)]
98. Zhou, Z.; Duan, K.; Wang, Z.; Liu, Z. Study on H<sub>2</sub>-SCR on Pd—Based catalyst. In Proceedings of the 11th National Conference on Environmental Catalysis and Environmental Materials, Chinese Chemical Society, Catalytic Committee of Chinese Chemical Society, Shenyang, China, 20–23 July 2018; pp. 1–5.
99. Chatziiona, V.K.; Constantinou, B.K.; Savva, P.G.; Olympiou, G.G.; Kapnisis, K.; Anayiotos, A.; Costa, C.N. Regulating the catalytic properties of Pt/Al<sub>2</sub>O<sub>3</sub> through nanoscale inkjet printing. *Catal. Commun.* **2018**, *103*, 69–73. [[CrossRef](#)]
100. Duan, K.; Liu, Z.; Li, J.; Yuan, L.; Hu, H.; Woo, S.I. Novel Pd–Au/TiO<sub>2</sub> catalyst for the selective catalytic reduction of NO<sub>x</sub> by H<sub>2</sub>. *Catal. Commun.* **2014**, *57*, 19–22. [[CrossRef](#)]
101. Hu, Z.; Yong, X.; Li, D.; Yang, R.T. Synergism between palladium and nickel on Pd–Ni/TiO<sub>2</sub> for H<sub>2</sub>-SCR: A transient DRIFTS study. *J. Catal.* **2020**, *381*, 204–214. [[CrossRef](#)]
102. Zhang, C.; Gao, Y.; Yan, Q.; Wang, Q. Fundamental investigation on layered double hydroxides derived mixed metal oxides for selective catalytic reduction of NO<sub>x</sub> by H<sub>2</sub>. *Catal. Today* **2020**, *355*, 450–457. [[CrossRef](#)]
103. Luo, Y.; Wang, X.; Qian, Q.; Chen, Q. Studies on B sites in Fe-doped LaNiO<sub>3</sub> perovskite for SCR of NO<sub>x</sub> with H<sub>2</sub>. *Int. J. Hydrogen Energy* **2014**, *39*, 15836–15843. [[CrossRef](#)]
104. Xue, Y.; Sun, W.; Wang, Q.; Cao, L.; Yang, J. Sparsely loaded Pt/MIL-96(Al) MOFs catalyst with enhanced activity for H<sub>2</sub>-SCR in a gas diffusion reactor under 80 °C. *Chem. Eng. J.* **2018**, *335*, 612–620. [[CrossRef](#)]
105. Yang, Q.; Chen, Z.; Zhou, D.; Shen, W.; Naito, S. Effect of cobalt substitution on nanoporous nickel phosphate VSB-5 catalyst for the catalytic reduction of NO by H<sub>2</sub>. *Catal. Today* **2017**, *297*, 64–69. [[CrossRef](#)]
106. Wang, L.; Yin, C.; Yang, R.T. Selective catalytic reduction of nitric oxide with hydrogen on supported Pd: Enhancement by hydrogen spillover. *Appl. Catal. A Gen.* **2016**, *514*, 35–42. [[CrossRef](#)]
107. Yin, C.; Zhao, Z. Preparation of a supported noble metal catalyst and its removal of NO<sub>x</sub> by H<sub>2</sub>-SCR. In Proceedings of the 16th National Industrial Catalytic Technology and Application Annual Conference, Tenzhou, China, 29 July–1 August 2019.
108. Ryou, Y.; Lee, J.; Cho, S.J.; Lee, H.; Kim, C.H.; Kim, D.H. Activation of Pd/SSZ-13 catalyst by hydrothermal aging treatment in passive NO adsorption performance at low temperature for cold start application. *Appl. Catal. B Environ.* **2017**, *212*, 140–149. [[CrossRef](#)]
109. Cao, L.; Wang, Q.; Yang, J. Ultrafine Pt particles directed by polyvinylpyrrolidone on zeolite beta as an efficient low-temperature H<sub>2</sub>-SCR catalyst. *J. Environ. Chem. Eng.* **2020**, *8*, 103631. [[CrossRef](#)]
110. Väliheikki, A.; Petalidou, K.C.; Kalamaras, C.M.; Kolli, T.; Huuhtanen, M.; Maunula, T.; Keiski, R.L.; Efstathiou, A.M. Selective catalytic reduction of NO<sub>x</sub> by hydrogen (H<sub>2</sub>-SCR) on WO<sub>x</sub>-promoted Ce<sub>2</sub>Zr<sub>1–2</sub>O<sub>2</sub> solids. *Appl. Catal. B Environ.* **2014**, *156*, 72–83. [[CrossRef](#)]

111. Kalamaras, C.M.; Olympiou, G.G.; Părvulescu, V.I.; Cojocaru, B.; Efstathiou, A.M. Selective catalytic reduction of NO by H<sub>2</sub>/C<sub>3</sub>H<sub>6</sub> over Pt/Ce<sub>1-x</sub>Zr<sub>x</sub>O<sub>2-δ</sub>: The synergy effect studied by transient techniques. *Appl. Catal. B Environ.* **2017**, *206*, 308–318. [[CrossRef](#)]
112. Liu, Z.; Lu, Y.; Yuan, L.; Ma, L.; Zheng, L.; Zhang, J.; Hu, T. Selective catalytic reduction of NO<sub>x</sub> with H<sub>2</sub> over WO<sub>3</sub> promoted Pt/TiO<sub>2</sub> catalyst. *Appl. Catal. B Environ.* **2016**, *188*, 189–197. [[CrossRef](#)]
113. Patel, V.K.; Sharma, S. Effect of oxide supports on palladium based catalysts for NO reduction by H<sub>2</sub>-SCR. *Catal. Today* **2020**. [[CrossRef](#)]
114. Wang, L.; Chen, H.; Yuan, M.-H.; Rivillon, S.; Klingenberg, E.H.; Li, J.X.; Yang, R.T. Selective catalytic reduction of nitric oxide by hydrogen over Zn-ZSM-5 and Pd and Pd/Ru based catalysts. *Appl. Catal. B Environ.* **2014**, *152–153*, 162–171. [[CrossRef](#)]
115. Olympiou, G.G.; Efstathiou, A.M. Industrial NO<sub>x</sub> control via H<sub>2</sub>-SCR on a novel supported-Pt nanocatalyst. *Chem. Eng. J.* **2011**, *170*, 424–432. [[CrossRef](#)]